

THE EFFECTS OF NITROGENATION LEVELS IN SPUTTERED CARBON OVERCOATS ON TRIBOLOGICAL PERFORMANCE IN ULTRA-HIGH VACUUM DRAG TESTS

by

Walton Fong, David B. Bogy, and C. Singh Bhatia

Abstract

A study on the effects of nitrogenation in sputtered, amorphous carbon overcoats (CN_x) on tribological performance in UHV drag tests is presented. To explain the phenomena observed in these tests, further characterization of the CN_x material properties and their interaction with ZDOL lubricant was carried out using the following techniques: (1) ESCA/XPS analysis, (2) Hysitron nano-scratch tests, and (3) Candela OSA lubricant mobility measurements. It was found that increasing the nitrogen content from 0 to 16 at. % in the carbon film effectively changes three properties at the head/disk interface: (1) it increases the wear resistance of the CN_x overcoat due to an increase in the sp^3/sp^2 ratio, (2) it decreases the surface mobility of ZDOL due to an increased dangling bond density in the carbon film, and (3) it decreases the catalytic decomposition of ZDOL in the presence of Al_2O_3 slider material. In UHV drag tests, the wear life of CN_x disk samples tested with DLC-coated sliders is governed by the first two properties, while tests with uncoated sliders are governed by all three.

1 Introduction

As a human civilization, we have accumulated approximately 12 exabytes (12×10^{18} bytes) of information in the last 300,000 years. However, with the advent of the internet and digital media applications, analysts predict that this number will double in the next 2.5 years [1]! To keep up with this blistering information growth, the need for storage is enormous. The areal densities of disk drive products have increased year after year at a rate of 100% since 1997 with no indications of decelerated growth in years to come [2]. Because Wallace's spacing loss equation dictates that the spacing between the read/write transducer on the head and the magnetic layer on the disk exponentially decreases as a function of areal density, the protective overcoats on these surfaces must be reduced also [3]. In fact, for 100 Gb/in^2 and 1 Tb/in^2 areal densities, recording performance models predict magnetic spacings of 10 and 6.5 nm, respectively [4, 5]. Overcoats on both the disk and slider, in turn, are on the order of 1 nm thick for the latter case!

Amorphous diamond-like carbon (DLC) films are popular choices as overcoat layers on these substrates and may be deposited by various techniques including DC magnetron sputtering [6-8], ion-beam deposition [9-11], and filtered cathodic-arc deposition [12-14]. Of particular interest to the disk drive industry is the use of sputtered DLC films as overcoats because the majority of media and head manufacturers would like to extend the life of existing sputtering tools in their process lines. However, at film thicknesses of 1 nm, sputtered carbon films may not possess the tribological properties required of a protective overcoat: (1) wear resistance, (2) corrosion protection, and (3) chemical compatibility with the lubricant.

Excellent wear resistance of the protective overcoat is a necessity -- with slider flyheight designs approaching 3.5 nm, intermittent contact between the head and the disk during normal operation is inevitable [15]. The addition of hydrogen and nitrogen to the carbon overcoat has allowed researchers to enhance the material properties of these DLC films for this need and much work has been published on this topic [7, 16-30]. Because of its properties, the use of CN_x films as a protective overcoat (5 to 10 nm thick) is widespread in the disk drive industry now and focus on developing thinner films without sacrificing performance continues today.

The magnetic alloy (usually a combination of cobalt, chromium, platinum, and other elements) used for the storage medium on disk media is highly susceptible to corrosion from the environment [3]. The oxides that form on this surface accumulate on the ABS and impair the stability of the slider's operation resulting in degradation of the readback signal and possibly failure of the HDI [31]. Hence, the need for an overcoat that acts as a barrier between the magnetic layer and the environment. Until recently, the porous nature of ultra-thin (< 5 nm) sputtered DLC overcoats prevented them from protecting the magnetic layers sufficiently, but by varying the deposition parameters during film preparation, researchers have been able to manipulate the microstructure of CN_x films extensively for various applications [25, 32, 33]. For disk drive applications, Guruz et. al demonstrated that by applying a pulsed bias voltage to the target and substrate during deposition, they were able to mono-energetically bombard the growing CN_x films and produce films as thin as 2 nm with excellent corrosion resistance [34]. With the addition

of substrate tilt and rotation, Li et. al were able to extend that level of corrosion protection to 1 nm films [35]. These latest developments with sputtered CN_x films make them a viable overcoat candidate for future disk drive products.

In addition to the increased mechanical interaction with low slider flyheights, the chemical reactions that occur at the HDI during those contacts are significant. The lubricant layer's role on the disk media is to reduce wear and friction during normal operation conditions and its durability must match that of the expected lifetime of the drive [3]. Lubricant evaporation, degradation, and diffusion are all factors that may be detrimental to the lifetime of the lubricant, especially in current disk media designs where the lubricant layer is only a few atoms thick, and they are influenced by their interaction with the underlying carbon surface. We use the term "tribochemistry" to describe these chemical interactions between the lubricant and carbon overcoat layers at the HDI and their effect on tribological performance [36]. The tribochemical studies of ZDOL, a popular PFPE lubricant for disk media, with carbon overcoats has led to the adoption of DLC-coatings on slider surfaces for extended life of the HDI. Kasai et. al showed how ZDOL lubricant decomposes differently in the presence of Al_2O_3 material versus pure thermal stimulation [37], and Yun et. al verified those findings in actual drag tests with disks and sliders (with and without DLC-coatings) in ultra-high vacuum [38]. Chen extended those studies to include the effects of various lubricant and overcoat parameters on drag life and lubricant decomposition [39]. Many others have conducted a myriad of experiments ranging from lubricant mobility measurements [40-42] to triboelectron-stimulated degradation of lubricant [43, 44] to in-situ monitoring of lubricant

redistribution in flyability tests [45, 46] – all with the express purpose of gaining insight into understanding the chemistry at the HDI. On the theoretical side, a large repository of work is available on models for lubricant and carbon overcoat interaction from Waltman [47-50], Kasai [51, 52], and others.

In this study, we investigate the effects of nitrogenation in sputtered DLC overcoats on the wear durability, friction, and lubricant decomposition in drag tests with an ultra-high vacuum tribochamber. Others have focused primarily on scratch-resistance of CN_x films or on the lubricant interaction with CN_x overcoats – it is our goal in this report to demonstrate the combined effects of lubricant decomposition and material properties of the CN_x films on actual drag tests with disks and sliders. Analysis of the CN_x overcoats and lubricant layers provide supporting evidence for the phenomena observed in these experiments.

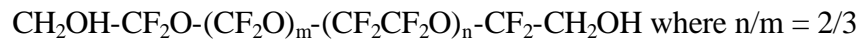
2 Experimental methods

2.1 Sample preparation

In this work, the disk samples were commercially-available, 65 mm aluminum disks with a “super-smooth” data zone (rms surface roughness of 0.349 nm). All samples were manufactured identically up to the carbon overcoat layer (i.e. plating, polish, texture, magnetic layer), whereupon an 11 nm CN_x overcoat was sputter-deposited with different nitrogen contents ranging from 0 to 16%. Processing of the CN_x overcoats was done by Richard L. White (IBM San Jose) in a commercial, single-disk sputter tool (BPS Circulus M12) with a base pressure of 3×10^{-7} Torr, using high purity graphite targets in Ar/N₂ gas

mixtures. To control the nitrogen percentage in the films, the partial pressure of N₂ was varied from 0 to 2 mTorr, while holding the total deposition pressure to approximately 6 mTorr. The deposition rate was ~ 1 nm/s. A total of five sets of CN_x overcoats with nitrogen contents of 0, 6, 9, 13.6, and 16% were fabricated. Nitrogen content in the CN_x overcoats was determined using Auger electron spectroscopy.

Upon completion of the CN_x overcoat process, all samples were lubricated with 1.4 nm of perfluoropolyether (PFPE) ZDOL by a dip-coating process and subjected to the same post-processing steps. The molecular weight of the ZDOL was 2000 AMU and its chemical formula is given below:



To insure uniform total lubricant thickness across the five sets of disks, the samples were drawn out of the lubricant bath at various pull rates ranging from 4.5 to 9.0 mm/s. Subsequently, a post-test measurement of all the disks revealed “bonded” lubricant thicknesses between 0.42 to 0.48 nm and “mobile” lubricant thicknesses ranging from 0.37 and 0.55 nm. Figure 1 gives the specific details for each cell. We defined the “bonded” lubricant as the portion remaining on the disk after a stripping process in a solvent bath. Subtracting the “bonded” lubricant thickness from the total lube thickness yielded the “mobile” lubricant contribution. All lubricant thicknesses were measured with Fourier transform infrared spectroscopy (FTIR) by Robert Waltman (IBM San Jose).

In addition to the disk samples, a second set of 5 nm CN_x overcoats was deposited on Si <100> wafer substrates with the full disk structure described earlier. These samples had nitrogen contents of 0, 6.5, 10.8, 16, and 20.5% in the CN_x overcoat. However, half the samples from each cell were lubricated at a constant pull rate of 1.7 mm/s, while the second half remained unlubricated. These samples were used in the nano-scratch tests and ESCA/XPS analysis.

2.2 X-Ray Photoelectron Spectroscopy (XPS) analysis

Surface analysis of the 5 nm CN_x samples with and without ZDOL lubricant was done with a Phi Quantum 2000 Electron Spectroscopy for Chemical Analysis (ESCA) system equipped with a monochromatic Al K α (1486.7 eV) x-ray source, which was operating at 99.7 W. Near-perpendicular (75°) and grazing (2°) photoelectron take-off angles were used to sample the bulk (characteristic sampling depth of 1.9 nm) and surface of the CN_x films, respectively. Also, both low- and high-resolution scans were done at corresponding analyzer pass energies of 58.70 and 29.35 eV with an aperture of 100 μ m. C 1s, O 1s, N 1s, F 1s, and Cr 3p spectra were collected for each sample.

2.3 Hysitron nano-scratch tests

Due to the thinness of the CN_x films under investigation, conventional nano-indentation tests for hardness and elastic modulus were not applicable. In addition, it was difficult to directly correlate such numbers with the wear durability of carbon films -- toughness of the material was a more relevant parameter. Thus, we evaluated the wear resistance of the

CN_x films in nano-scratch tests, where diamond tips were used to scratch test surfaces at very light loads to gauge their resistance to wear.

The Hysitron system [53] is a portable add-on to commercially available atomic force microscopes (AFM). We used a Digital Instruments Nanoscope III in our laboratory. The Hysitron lateral force transducer is centered around a capacitive force/displacement sensor that provides high sensitivity, a large dynamic range, and a linear force/displacement output signal. In these nano-scratch tests, we utilized the 5 nm CN_x films deposited on the Si wafers. A Berkovich diamond tip with a nominal radius of 331 nm was used to make 2 μm long scratches into the sample surface with a ramped loading force of 100 μN. Figure 2 shows the loading force and lateral displacement of the tip over the surface for each scratch. Before and after the nano-scratch tests, 200 μN indents were made into a reference fused quartz surface to confirm no changes or damage to the diamond tip shape. The TriboScope 3.5FL software was used to specify the scratch test parameters, record load/displacement data during scratching, and analyze data afterwards.

2.4 Candela Optical Surface Analyzer (OSA) lubricant mobility measurements

As mentioned earlier, the mobility of the lubricant on a disk's surface is a significant factor in the tribology of the head-disk interface. Good lubricant mobility allows the re-flow of lubricant to areas of the disk surface where head-disk contacts may have removed the lubricant temporarily. This occurs during the contact-start-stop cycles of disk drives that do not utilize load/unload technology and, more recently, during flying/seeking over the data zone with low flyheight slider designs. However, too much mobility is

detrimental to the overall life of the HDI, as spin-off of the lubricant prevents it from protecting the overcoat surface. This is becoming increasingly important as spindle speeds in current disk drives are 15,000 rpm and expected to go higher.

Lubricant mobility is a function of the interaction between the lubricant molecules and the carbon overcoat surface. Although there is no consensus on the exact specifics of this lubricant/carbon interaction, we expect changes in the carbon overcoat composition to affect its surface properties such as surface energy and dangling bond density, and hence its interaction with the lubricant molecule.

The Candela Optical Surface Analyzer (OSA) is a commercially-available measurement system capable of ellipsometry, reflectometry, scatterometry, and Kerr effect microscopy for imaging and metrology applications related to the inspection of disk media. The system was originally designed by Meeks et. al for in-situ imaging and analysis of the surface of a thin film disk, specifically lubricant depletion/degradation and carbon wear [54].

In our laboratory, we utilize a modified Candela 5100 OSA system that allows the use of additional fixtures and stages to mount HGAs for dynamic studies and in-situ monitoring of the head-disk interface. Several data channels may be monitored including P and S polarized light, Q polarized light (comprised of both P and S polarized light components), the M channel for magnetic characterization, and the Z channel for topology measurements. For lubricant thickness measurements, the Q polarized light channel

offers the most sensitivity with a resolution of 0.1\AA and works on the principal of ellipsometry – the instrument measures the phase shift between the P and S components of a Q polarized wave before and after it reflects off the sample surface. The difference is what is recorded in the phase shift image and is affected by the multi-layers of the disk sample including the lubricant and carbon overcoat.

Samples were prepared prior to test by removing the mobile lubricant from a radial track of the disk surface with a swab soaked in 3M HFE-7100 solvent, which is commonly used to strip disks of their lubricant layer. A fixture was designed to insure the track was straight and repeatable between samples. With the Candela TS software version 2.3.9, we acquired the QAbsPhase channel data at 5 minute intervals from a 2 mm by 30° angular section of the test track located at a radius of 26 to 28 mm. The total test duration was 15 hours and the disk was stationary between measurements to reduce the effects of centrifugal force and air shear on lubricant movement. Using the following parameters, our spatial resolution was $3.7\ \mu\text{m}$ in the radial direction and $2.6\ \mu\text{m}$ in the circumferential direction: 10,000 rpm spindle speed, “medium” resolution setting, 64X encoder multiplier, 10.923 MHz sample rate, 541 tracks, and 5482 pixels/track. The measured images are subtracted from the initial image ($t=0$) to insure that the only differences observed are due to the lubricant and none of the other underlying films on the disk surface (i.e. carbon overcoat). An angular average of the data over the sample area is calculated to provide a cross-section of the test track with increased signal/noise ratio. Finally, plotting this data as a function of time allows us to monitor the flow of lubricant back into the test track.

2.5 Ultra-high vacuum (UHV) tribochamber drag tests

The UHV tribochamber consists of a disk spindle, a slider actuator, a substrate heater, and a Balzers QMG 420 high-resolution quadrupole mass spectrometer (QMS) in a stainless-steel vacuum chamber. A base pressure of less than 2×10^{-8} Torr was achieved through the use of a Balzers TPU 330 turbo-molecular pump that was backed by a Balzers DUO 016B mechanical pump. The chamber pressure was monitored with two Varian gauges: a 524-2 cold cathode ionization gauge and a UHV-24 Bayard-Alpert type ionization gauge. The disk spindle was driven by a DC motor at rotational speeds of 50 to 64 rpm through a UHV-compatible feedthrough. A slider was mounted on the slider actuator, which has a strain arm instrumented with semiconductor strain gauges to measure forces in the vertical and horizontal directions, and its XYZ position was controlled via linear stages. More specific details of this system were described in an earlier CML report [55].

The QMS provided in-situ detection of the gaseous products generated at the HDI during drag tests. The QMS can monitor simultaneously 15 different atomic mass units (AMUs) ranging from 1 to 500. We simultaneously obtained friction data from strain gauge transducers. Based on earlier work [55], specific AMUs were monitored during drag tests to examine the decomposition mechanisms of ZDOL: 2 (H_2), 12 (C), 19 (F), 20 (HF), 28 (N_2 or CO), 31 (CF), 44 (CO_2), 47 (CFO), 50 (CF_2), 51 (CF_2H), 66 (CF_2O), 69 (CF_3), 100 (C_2F_4), 116 (C_2F_4O), and 119 (C_2F_5).

The following test procedure was used to conduct drag tests in the tribochamber. Initially, the tribochamber was heated to 423 K at high vacuum for 24 hours. The chamber was then backfilled with Argon gas as the disk and slider samples were mounted inside. The sliders used in this study were 30% (1.25 mm by 1 mm) Al₂O₃-TiC sliders with and without 7 nm amorphous diamond-like carbon (DLC) films on their air bearing surfaces (ABS). Next, the chamber was pumped down to a base pressure of 2×10^{-8} Torr and the channels of the QMS were assigned to the selected AMUs. The background intensities were recorded before the drag tests were initiated with the following parameters: 0.2 m/s drag speed, a load of 2.5 grams, and a sliding time until failure. The mass spectrum and friction data were collected every 2 seconds by a computer connected to the QMS via a serial connection.

3 Results and discussion

3.1 X-ray Photoelectron Spectroscopy (XPS) analysis

The first analysis was conducted on the unlubricated 5 nm CN_x films with near-perpendicular take-off angles (75°) to examine the bulk structure of the overcoats. Figures 3 through 5 correspond to the C1s, O1s, and N1s high-resolution spectra, respectively. In Figure 3, we noted a broadening of the C1s spectrum with the addition of nitrogen to the overcoats – this pattern was expected as more highly nitrogenated C moieties formed at higher nitrogen concentrations in the overcoat. Unfortunately, this broadening of the C1s spectrum makes it impossible to deconvolute the peaks that correspond to various C-N bonds such as those found in β-C₃N₄ and graphitic C₃N₄ structures. Instead, we turn to the N1s spectra in Figure 5, where increasing the nitrogen

content of the overcoats correlated with the relative change of two distinct peaks in the $N1s$ spectrum at 398.5 eV and 400.5 eV. The unambiguous assignment of all the peaks observed in this spectrum to specific film microstructures is nearly impossible, but a useful compilation by Hellgren [33] of the published work in this field (both experimental and theoretical) allowed us to identify these two features. The 400.5 eV peak corresponds to nitrogen bonded to sp^2 -coordinated carbon in an aromatic structure, whereas the 398.5 eV peak may be associated with nitrogen bonded to sp^3 -coordinated carbon. Hence, the ratio of these two peaks provides an indication of the sp^3/sp^2 content in the CN_x films and we observed that increasing the nitrogen in the overcoats corresponded to an increase of the sp^3 content in the films.

Analysis of the lubricated 5 nm CN_x samples provided information about the lubricant's bonding behavior to the carbon surface. Figures 6 through 8 are the $F1s$, $C1s$, and $O1s$ low-resolution spectra, respectively, taken at near-perpendicular take-off angles (75°). From the $F1s$ spectra and the peaks on the left-hand side of the $C1s$ and $O1s$ spectra (associated with the lubricant), we noted no significant change in the lubricant's structure as a function of nitrogen content in the overcoat. Also, the lubricant thickness did not vary with the addition of nitrogen to the overcoat as it ranged from 14.19 to 14.98 Å.

3.2 Hysitron nano-scratch tests

Figure 9 is a plot of the normal displacement vs. time for a scratch on the 0% N_2 overcoat sample, which was representative of the data taken with this instrument. The tilt of the sample, due to mounting and other set-up errors, was taken into consideration and

subtracted from the data using the software functions. Since we had clearly scratched through the carbon film layer and into the underlying substrate layers with a load of 100 μN , we chose to compare the normal displacement at a load of 5 μN for each of the overcoat samples to evaluate the scratch resistance of the carbon films. A summary of the results is plotted in Figure 10 as a function of % N_2 in the overcoat. Each data point is the average of eight measurements.

The normal displacement we measured in these nano-scratch tests included the effects of both elastic and plastic deformation of the sample surface. As the nitrogen content in the CN_x overcoat was increased above 6%, we observed an increase in the scratch resistance of the carbon film as exhibited by the decrease in the tip's normal displacement into the sample surface. Further addition of nitrogen into the overcoat past 16% resulted in no appreciable increase in scratch resistance. Our results matched those reported by Wiens et. al, where they conducted scratch tests on similar samples with a normal load of 3 μN in their scanning force microscope (SFM) [56]. Using Raman spectroscopy to observe the shift of the *G*-peak position, they attributed the increased scratch resistance to increased sp^3 bonding in the carbon films. In our own XPS analysis described earlier, we also observed an increase in sp^3 bonding as a function of nitrogen content in the carbon overcoat. In addition to improved scratch resistance, this change in the carbon film's microstructure has been correlated to increases in hardness and elastic modulus, density, and other material properties [25,26].

3.3 Candela Optical Surface Analyzer (OSA) lubricant mobility measurements

Figure 11 is a typical QAbsPhase image taken immediately after removing the lubricant from the test track – this one corresponds to the surface of the 18% N₂ disk. Brighter colors on the image (the light vertical strip) indicate less lubricant in the test track, while the darker hues represent the normal lubricant thickness on the disk. An angular average of the test area is shown in Figure 12 for this disk. As can be seen from the plot, averaging the data over the test area allows us to quantify the amount of lubricant in and out of the test track. Positive reflectivity values indicate less lubricant on the disk. By subtracting this original image from all the subsequent measurements, we arrive at the plot shown in Figure 13 of the reflectivity difference at the test track (positive differences indicate more lubricant on the disk surface in this plot). As time progresses, the lubricant slowly re-flows back to the test track from the surrounding areas.

To study the effects of nitrogenation in the overcoat on lubricant mobility, we compared the integrated intensities of the test track reflectivity differences for low nitrogen (9.5 at. %) and high nitrogen (18 at. %) CN_x disks as a function of time. In Figure 14, we observe that more lubricant re-flows into the test track for the low nitrogen disk – hence, the surface mobility of ZDOL decreases as the amount of nitrogen in the overcoat increases. Ma et. al noted similar results in their micro-ellipsometry studies of ZDOL spreading on amorphous carbon surfaces with hydrogen and nitrogen doping [42]. These experimental results were later confirmed in their theoretical model involving the solution of the two-dimensional diffusion equation using the finite-difference method [57].

The surface mobility of ZDOL is dependent upon the number of adsorption sites on the carbon film surface where the lubricant molecule may interact or bond – for hydrogenated amorphous carbon films (CH_x), this was shown to be carboxyl end groups (COOH) and dangling bonds (unpaired electrons) based on XPS and electron spin resonance (ESR) studies [40]. Increasing the number of these high-energy bonding sites provides places for the lubricant molecules to anchor themselves and, effectively, reduce their motion over the carbon surface. For dangling bonds in the carbon film, Kasai demonstrated that ZDOL attaches itself via the transfer of a hydrogen atom from the active hydroxyl endgroup to a dangling bond site, linking the molecule as an alkoxy group [58]. From our XPS analysis, we found that increasing the nitrogen content of CN_x overcoats increases the amount of sp^3 -coordinated C in the films. This data may be coupled with the fact that the dangling bond density of carbon surfaces correlates with the sp^3 content of the sample, as observed by Yanagisawa in his ESR studies [59], to infer that increasing the N_2 content of films increases the dangling bond density on the CN_x overcoat. It is this increase in the dangling bond density that results in the decreased surface mobility of the ZDOL lubricant as a function of nitrogen content in the overcoat. Other detailed mechanisms proposed for the bonding of the ZDOL hydroxyl endgroups and its ether linkages to nitrogenated carbon surfaces may be found in work by Tyndall et. al and Paserba et. al [60, 61].

3.4 UHV tribochamber drag tests

Figure 15 shows a plot of the friction coefficient vs. drag time for the 0% N_2 overcoat case tested with uncoated and 7 nm DLC-coated sliders, which is representative of the

data taken from the strain gauge transducer. From this friction data we extracted two sets of information: (1) the maximum friction coefficient observed at the head-disk interface (HDI) during the test and (2) the time of failure of the HDI, which is marked by a rapid drop in the friction along with the formation of a wear track on the disk. Compiling the data from each of these tests into summary plots allowed us to discern any trends with N_2 content in the overcoats.

Figure 16 is a plot of wear life vs. N_2 content in the overcoat for tests with the DLC-coated sliders; a similar plot for drag tests with the uncoated sliders is shown in Figure 17. In tests with the DLC-coated sliders, we noted a peculiar trend in wear life that was neither monotonically increasing nor decreasing as a function of % N_2 in the overcoat. Hence, we tested these samples again except in reverse order (i.e. from 16% to 0 %, whereas the first set of tests were from 0% to 16%) and acquired a similar set of data points. For the uncoated slider tests, we observed an increase in wear durability for nitrogen content in the overcoats greater than 9%.

A summary of the maximum friction coefficient observed in each test is presented in Figure 18. No changes in the friction coefficient were observed as a function of % N_2 in the overcoat in tests with the DLC-coated sliders. However, we noted a drop in the maximum friction coefficient as the N_2 content of the overcoat exceeded 9%.

A post-test analysis was done of the slider ABS under an optical microscope at 50X magnification for each test. A summary of the results is shown in Figure 19 for both the

DLC-coated and uncoated sliders. Even though comparisons of the amount or type of debris on the slider ABS are subjective in nature, we noted a visual difference in the debris composition from tests on disks with different % N₂ overcoats. Sliders from tests on the lower % N₂ overcoats had debris that consisted of smears or liquid-like material, whereas sliders from tests with high % N₂ overcoats had particulate-like debris embedded on the rail surfaces. The change in the overcoat from an sp²- to sp³-rich microstructure with the addition of nitrogen to the overcoat, as observed in the XPS analysis, may account for this transition in debris generation.

Figure 20 is a summary of the mass spectra taken from the QMS for drag tests on the 0% N₂ overcoat disk with DLC-coated and uncoated sliders, which is representative of the data taken with this instrument. Four mass fragments were monitored specifically to determine the extent of the ZDOL lubricant decomposition that occurs at the HDI during these drag tests: CFO (47 a.m.u.), CF₂O (66 a.m.u.), CF₃ (69 a.m.u.), and C₂F₅ (119 a.m.u.). We categorized the decomposition of ZDOL lubricant into two mechanisms, a thermal decomposition or mechanical scission of the molecule and a catalytic decomposition. CFO and CF₂O are associated with the thermal decomposition or mechanical scission of the lubricant molecule due to friction generated at the HDI. CF₃ and C₂F₅ are the end products of the catalytic decomposition of ZDOL in the presence of slider material Al₂O₃-TiC. A complete outline of the decomposition mechanisms may be found elsewhere [36].

For the DLC-coated slider case, we observed the immediate generation of CFO and CF₂O at the beginning of the drag test, which coincided with the initiation of friction. As the test progressed, the intensity of these fragments declined as the amount of lube available for this decomposition mechanism was depleted from the wear track. Finally, catastrophic failure of the HDI occurred when the amount of lubricant could no longer protect the overcoat and the carbon film was worn away. Insignificant amounts of CF₃ and C₂F₅ were observed because the DLC-coating on the slider surface prevented any interaction between the Al₂O₃-TiC material and the lubricant on the disk.

For the uncoated slider case, friction at the HDI initiated the generation of CFO and CF₂O similar to the DLC-coated slider case. However, at the same time, we noted the production of CF₃ and C₂F₅, indicating the presence of the catalytic decomposition mechanism. As this decomposition progressed, the intensities of these fragments continued to increase – a similar trend was also observed in the CFO and CF₂O spectra because (1) these fragments are also generated in small amounts as a by-product of the catalytic decomposition, and (2) the friction at the interface increased significantly. Failure of the HDI took place when carbon wear occurred after the lube was depleted from the test track.

Therefore, the dominant lubricant decomposition mechanism for tests with DLC-coated sliders is a thermal decomposition or mechanical scission of the molecule. For tests with uncoated sliders, it is the catalytic decomposition that dictates the lifetime of the lubricant. To determine the effects of overcoat nitrogenation on lubricant decomposition,

we need a method of quantifying the extent of these two mechanisms. First, we integrate the intensity of each mass fragment over the duration of each individual test to determine the overall amount of lubricant decomposition that occurred at the HDI. Figures 21 through 24 show the integrated spectra for CFO, CF₂O, CF₃, and C₂F₅, respectively, as a function of nitrogen content in the overcoats when tested with DLC-coated and uncoated sliders. From these plots, we observe that less lubricant is decomposed at the HDI as the nitrogen content increases in the carbon overcoat. This stems from the fact that the surface mobility of ZDOL decreases with increasing nitrogen content based on our Candela measurements -- more lubricant re-flows back into the test track of samples with lower nitrogen overcoats providing more material to participate in the decomposition, which results in more mass fragments being generated and counted by the quadrupole mass spectrometer. For the uncoated slider case, where failure times were fairly short, the effects of lubricant re-flow are most likely minimal, and the substantial decrease in the catalytic decomposition at higher % N₂ in the overcoat may be attributed to other factors.

One possible scenario for the reduced catalytic decomposition is based on the bonding characteristics of the ether linkages in the ZDOL backbone to the carbon film and supported by our work with hydrogenated and nitrogenated carbon overcoats in the UHV tribochamber. Paserba et. al indicated in their temperature-programmed desorption experiments that ethers interact with carbon films through electron donation from the oxygen lone pair electrons [61]. Nitrogen is electronegative relative to carbon and its addition to a carbon film depletes electrons from the film - hence, enhancing the bonding between the ZDOL ether linkages and the carbon surface. For hydrogen, which is

electropositive relative to carbon, its addition to carbon films donates electrons to the film, which weakens the ether bonding [62]. Evidence of the effects of this bonding mechanism on the catalytic decomposition may be found in drag tests with uncoated sliders in our UHV tribochamber. In Chen's dissertation [39], the addition of hydrogen to carbon overcoats resulted in an increase in the catalytic decomposition of ZDOL in drag tests with uncoated sliders and he suggests that it is the presence of acetal units, $-O-CF_2-O-$, in ZDOL that is the source of the decomposition, but he does not elaborate on the specifics. As can be seen from our explanation, the addition of hydrogen weakens the ether bonding at the carbon/lubricant interface resulting in increased catalytic decomposition of the ZDOL backbone, explaining Chen's results, while the addition of nitrogen enhances this bonding mechanism, reducing the catalytic decomposition in our results. Thus, increasing the % N_2 in the carbon overcoat reduces the catalytic decomposition in the presence of Al_2O_3 material.

Since the comparison of the integrated intensity does not take into account the disparate time scales to failure (hours versus minutes), it does not present an accurate picture of the severity of these decomposition mechanisms. For instance, in the 0% N_2 case, tests with the uncoated and the DLC-coated slider resulted in a similar "amount" of CFO mass fragments produced at the HDI, suggesting no significant difference between the two sliders, but the uncoated slider case produced that "amount" in 1/30th of the time of the DLC-coated slider test case – a significant factor to consider in this comparison. To incorporate this temporal dependence in our analysis, a more appropriate "number" to compare this set of data was an "average decomposition rate", which was the integrated

mass spectrum for each fragment normalized by the time to failure. This is comparable to plotting the average mass fragment intensity generated per revolution of sliding on the disk surface.

Figures 25 through 28 are the average decomposition rates for CFO, CF₂O, CF₃, and C₂F₅, respectively, as a function of nitrogen content in the overcoats when tested with DLC-coated and uncoated sliders. The trends are similar to those observed in Figures 21 through 24, but now we can clearly see how much more aggressive the catalytic decomposition process is compared to the thermal decomposition/mechanical scission at the HDI. The decomposition rates for the uncoated sliders were one order of magnitude higher than the DLC-coated sliders, which give an indication as to how long the interface lasted before failure in each test. Until recently, most sliders in disk drive products were coated with a significant amount of DLC that insured the isolation of the Al₂O₃ material on the slider from the lubricant on the disk surface. With the push for reduced magnetic spacing, this coating has been reduced (< 5 nm) and our tests have shown that at these levels, the DLC coatings may be worn off, exposing the Al₂O₃ material and initiating this more devastating decomposition mechanism. This is a significant concern for future products as the catalytic decomposition of ZDOL lubricant will shorten the life expectancy of the HDI.

In addition to these drag tests, a 2nd series of tests were conducted with similar CN_x disks, but WITHOUT the lubricant layer. Obviously, the removal of the lubricant from the disk structure isolates only the material properties of the overcoat in determining the

wear life of the HDI. Figure 29 is a plot of the wear durability vs. nitrogen content for these disks tested with DLC-coated and uncoated sliders. From this data, it is clear that increasing the % N₂ in the overcoat improved its resistance to wear via sliding. This data correlates well with the improved scratch resistance demonstrated in the Hysitron nano-scratch test results and may be explained by the increase in sp³ content of the carbon film from our XPS analysis.

Incorporating our myriad of results into a simple schematic, as shown in Figure 30, we can finally explain the drag test trends observed in the UHV tribochamber. Increasing the nitrogen content in the CN_x overcoat effectively changes two properties of the carbon film: (1) increased wear resistance of the overcoat itself, as demonstrated by unlubricated CN_x disk drag tests, Hysitron nano-scratch tests, and XPS analysis, and (2) decreased surface mobility of ZDOL lubricant due to an increase in the dangling bond density.

For the uncoated slider case, increasing the % N₂ in the overcoat improved wear durability because the aggressive nature of the catalytic decomposition negated any benefits of improved ZDOL surface mobility, and only the wear resistance of the carbon films was reflected in the trends.

For the DLC-coated slider case, the superposition of these two phenomena resulted in our observations as shown in Figure 30. At low nitrogen concentrations, the surface mobility of the ZDOL lubricant is enhanced which allows for replenishment of the wear track after the slider passes over the disk and provides continued protection of the overcoat layer.

Since the scratch resistance of the overcoat itself is not optimal in this regime, it is the lubricant layer that plays the dominant role in determining wear life. As the N₂ content is further increased in the overcoat, ZDOL mobility decreases and we observe a decrease in wear life. A transition occurs at approximately 9% N₂ content though – the ZDOL mobility continues to decrease, but the inherent scratch resistance of the overcoat increases and becomes the source of the improved wear durability noted at the HDI for higher N₂ concentrations. Because no catalytic decomposition of the lubricant is observed in these tests with DLC-coated sliders, only the thermal decomposition/mechanical scission of the lubricant is possible. The rate of this reaction is comparable among the disks, as the friction at the HDI is similar for these series of tests, so we neglect any contributions from lubricant decomposition in this explanation.

4 Conclusions

The effects of nitrogenation in sputtered, amorphous carbon overcoats (CN_x) on tribological performance in UHV drag tests were investigated. In this report, we demonstrated that increasing the nitrogen content from 0 to 16% effectively changes three properties at the head/disk interface: (1) increases the wear resistance of the CN_x overcoat due to an increase in the sp³/sp² ratio as observed by Hysitron nano-scratch tests, ESCA/XPS analysis, and drag tests with unlubricated disk samples, (2) decreases the surface mobility of ZDOL due to an increased dangling bond density in the carbon film, and (3) decreases the catalytic decomposition of ZDOL in the presence of Al₂O₃ slider material. In UHV drag tests, the wear life of CN_x disk samples tested with DLC-

coated sliders is governed by the first two properties, while tests with uncoated sliders are governed by all three.

5 Acknowledgments

We would like to thank Richard L. White for preparing the CN_x overcoats on the various substrates, Robert Waltman for providing the lubrication and post-processing of the samples, Mike Suk for enlightening us on the benefits and shortcomings of the Candela system, and Daryl Pocker for the insightful ESCA/XPS analysis and discussion, all of them from IBM in San Jose. This work was supported by the National Storage Industry Consortium and the Computer Mechanics Laboratory.

6 References

- [1] Coughlin, T. and Wald, D., "SANs/SSPs Drive Storage Demand," *DATA Storage*, February 2001.
- [2] Grochowski, E., "IBM Leadership in Disk Storage Technology," <http://www.almaden.com/sst/html/leadership/g02.htm>.
- [3] Mee, C. and Daniel, E., *Magnetic Recording Handbook: Technology & Applications*. United States of America: McGraw-Hill, Inc, 1990.
- [4] Bhatia, C. S., Polycarpou, A. A., and Menon, A., *Forward of Proceedings of the Symposium on Interface Tribology Towards 100 Gb/in² and Beyond*, ASME Trib-Vol. 10, Seattle, WA, Oct. 2000, p. iii.
- [5] Wood, R., "The Feasibility of Magnetic Recording at 1 Terabit per Square Inch," *IEEE Transactions on Magnetics*, Vol. 36, No. 1, January 2000, pp. 36-42.
- [6] Tsai, H. and Bogy, D. B., "Characterization of Diamondlike Carbon Films and Their Application as Overcoats on Thin-film Media for Magnetic Recording," *J. Vac. Sci. Technol. A*, Vol. 5, No. 6, November/December 1987, pp. 3287-3312.
- [7] Huang, L., Hung, Y., and Chang, S., "Structure of Nitrogenated Carbon Overcoats on Thin-Film Hard Disks," *IEEE Transactions on Magnetics*, Vol. 33, No. 6, November 1997, pp. 4551-4559.
- [8] Sivertsen, J. M., Wang, G., Chen, G., and Judy, J., "Evaluation of Amorphous Diamond-Like Carbon-Nitrogen Films as Wear Protective Coatings on Thin Film Media and Thin Film Head Sliders," *IEEE Transactions on Magnetics*, Vol. 33., No. 1, January 1997, pp. 926-931.
- [9] Bhushan, B., "Chemical, Mechanical and Tribological Characterization of Ultra-thin and Hard Amorphous Carbon Coatings as Thin as 3.5 nm: Recent Developments," *Diamond and Related Materials*, Vol. 8, 1999, pp. 1985-2015.
- [10] Akita, N., Konishi, Y., Ogura, S., Imamura, M., Hu, Y. H., and Shi, X., "Comparison of deposition methods for ultra thin DLC overcoat film for MR head," *Diamond and Related Materials*, Vol. 10, 2001, pp. 1017-1023.
- [11] Druz, B., Zaritskiy, I., Hoehn, J., Polyakov, V. I., Rukovichnikov, A. I., and Novotny, V., "Direct ion beam deposition of hard (>30 GPa) diamond-like films from RF inductively coupled plasma source," *Diamond and Related Materials*, Vol. 10, 2001, pp. 931-936.
- [12] Fong, W., "Fabrication and evaluation of 5 nm cathodic-arc carbon films for disk drive applications," *M.S. Project Report 99-002 (Gold Series)*, Computer Mechanics Laboratory, University of California, Berkeley, CA, October 1999.
- [13] Anders, A., Fong, W., Kulkarni, A., Ryan, F., and Bhatia, C. S., "Ultrathin Diamond-like Carbon Films Deposited by Filtered Cathodic Arcs," accepted for publication in *IEEE Transactions on Plasma Sciences*, Vol. 29, No. 5, 2001.
- [14] Anders, S., Bhatia, C. S., Fong, W., Lo, R., Bogy, D. B., "Application of cathodic-arc deposited amorphous hard carbon films to the head/disk tribology," *Materials Research Society Symposium Proceedings, High-Density Magnetic Recording and Integrated Magneto-Optics: Materials and Devices*, Vol. 517, 1998, pp. 371-382.

- [15] Thornton, B. H., Nayak, A., and Bogy, D. B., "Flying Height Modulation Due to Disk Waviness of Sub-5nm Flying Height Air Bearing Sliders," *Journal of Tribology*, accepted for publication.
- [16] Marchon, B., Vo, P. N., Khan, M. R., and Ager III, J. W., "Structure and Mechanical Properties of Hydrogenated Carbon Films Prepared by Magnetron Sputtering," *IEEE Transactions on Magnetics*, Vol. 27, No. 6, November 1991, pp. 5160-5162.
- [17] Lee, H. J., Zubeck, R., Hollars, D., Lee, J. K., Smallen, M., and Chao, A., "Material Properties and Tribological Performance of Hydrogenated Sputter Carbon Overcoat on Rigid Disk," *J. Vac. Sci. Technol. A.*, Vol. 11, No. 6, November/December 1993, pp. 3007-3013.
- [18] Lee, J. K., Smallen, M., Enguero, J., Lee, H. J., and Chao, A., "The Effect of Chemical and Surface Properties of Hydrogenated Carbon Overcoats on the Tribological Performance of Rigid Magnetic Disks," *IEEE Transactions on Magnetics*, Vol. 29, No. 1, January 1993, pp. 276-281.
- [19] Lal, B. B., Yang, M., Chao, J., and Russak, M. A., "Asymmetric DC-Magnetron Sputtered Carbon-Nitrogen Thin-Film Overcoat for Rigid-Disk Applications," *IEEE Transactions on Magnetics*, Vol. 32., No. 5, September 1996, pp. 3774-3776.
- [20] Cutiongco, E. C., Li, D., Chung, Y. W., and Bhatia, C. S., "Tribological Behavior of Amorphous Carbon Nitride Overcoats for Thin-Film Rigid Disks," *Journal of Tribology*, Vol. 118, July 1996, pp. 543-548.
- [21] Wang, R. H., Meeks, S. W., White, R. L., Weresin, W. E., "The Effect of Hydrogen in Carbon Overcoats on the Tribology of the Head-Disk Interface," *IEEE Transactions on Magnetics*, Vol. 31, No. 6, November 1995, pp. 2919-2921.
- [22] Agarwal, S., Li, E., and Heiman, N., "Structure and Tribological Performance of Carbon Overlayer Films," *IEEE Transactions on Magnetics*, Vol. 29, No. 1, January 1993, pp. 264-269.
- [23] White, R. L., Bhatia, S. S., Friedenber, M. C., Meeks, S. W., and Mate, C. M., "RF-Sputtered Amorphous CN_x for Contact Recording Applications," *Tribology of Contact/Near-Contact Recording for Ultra High Density Magnetic Storage*, TRIB-Vol. 6, 1996, pp. 33-38.
- [24] Bhushan, B. and Koinkar, V. N., "Microscale Mechanical and Tribological Characterization of Hard Amorphous Carbon Coatings as Thin as 5 nm for Magnetic Disks," *Surface and Coatings Technology*, Vol. 76-77, 1995, pp. 655-669.
- [25] Broitman, E., Hellgren, N., Wänstrand, O., Johansson, M. P., Berlind, T., Sjöström, H., Sundgren, J. E., Larsson, M., and Hultman, L., "Mechanical and Tribological Properties of CN_x Films Deposited by Reactive Magnetron Sputtering," *Wear*, Vol. 248, 2001, pp. 55-64.
- [26] Lu, W. and Komvopoulos, K., "Dependence of Growth and Nanomechanical Properties of Ultrathin Amorphous Carbon Films on Radio Frequency Sputtering Conditions," *Journal of Applied Physics*, Vol. 86, No. 4, August 1999, pp. 2268-2277.
- [28] Ott, R. D., Scharf, T. W., Yang, D., and Barnard, J. A., "Tribological and Mechanical Properties of CN Ultra-Thin Overcoat Films," *IEEE Transactions on Magnetics*, Vol. 34, No. 4, July 1998, pp. 1735-1737.
- [29] Scharf, T. W., Ott, R. D., Yang, D., and Barnard, J. A., "Structural and Tribological Characterization of Protective Amorphous Diamond-like Carbon and Amorphous CN_x Overcoats for Next Generation Hard Disks," *Journal of Applied Physics*, Vol. 85, No. 6, March 1999, pp. 3142-3154.

- [30] Wienss, A., Neuhäuser, M., Schneider, H. H., Persch-Schuy, G., Windeln, J., Witke, T., and Hartmann, U., "Mechanical Properties of D.C. Magnetron-Sputtered and Pulsed Vacuum Arc Deposited Ultra-Thin Nitrogenated Carbon Coatings," *Diamond and Related Materials*, Vol. 10, 2001, pp. 1024-1029.
- [31] Chia, R. W. J., Wang, C. W., Lee, J. J. K., and Tang, W. T., "Overview of corrosion on thin film magnetic media and its implication on head disk interface," *Proceedings of the Fifth International Symposium on Magnetic Materials, Processes, and Devices Applications to Storage and Microelectromechanical Systems (MEMS), Boston, MA, Nov. 1-6, 1998*. Pennington, New Jersey: Electrochem. Soc, 1999, pp. 255-68.
- [32] Sjöstrom, H., Hultman, L., Sundgren, J. E., Hainsworth, S. V., Page, T. F., and Theunissen, G. S. A. M., "Structural and Mechanical Properties of Carbon Nitride CN_x (0.2 ≤ x ≤ 0.35) Films," *J. Vac. Sci. Technol. A*, Vol. 14, No. 1, January/February 1996, pp. 56-62.
- [33] Hellgren, N., "Sputtered Carbon Nitride Thin Films," *Linköping Studies in Science and Technology, Dissertation No. 604, Linköping University, Sweden 1999*.
- [34] Guruz, M. U., Dravid, V. P., Chung, Y. W., Lacerda, M. M., Bhatia, C. S., Yu, Y. H., and Lee, S. C., "Corrosion Performance of Ultrathin Carbon Nitride Overcoats Synthesized by Magnetron Sputtering," *Thin Solid Films*, Vol. 381, 2001, pp. 6-9.
- [35] Li, D., Guruz, M. U., and Chung, Y. W., "Ultrathin CN_x Overcoats for 1 Tb/in² Hard Disk Drive Systems," submitted for publication.
- [36] Bhatia, C. S., Fong, W., Chen, C. Y., Wei, J., Bogy, D. B., Anders, S., Stammeler, T., Stöhr, J., "Tribo-chemistry at the Head/Disk Interface," *IEEE Transactions on Magnetics*, Vol. 35, No. 2, Part 1, March 1999, pp. 910-915.
- [37] Kasai, P. H., Tang, W. T., Wheeler, P., "Degradation of Perfluoropolyethers Catalyzed by Aluminum Oxide," *Applied Surface Science*, Vol. 51, September 1991, pp. 201-211.
- [38] Yun, X., Bogy, D. B., and Bhatia, C. S., "Wear of Hydrogenated Carbon Coated Disks by Carbon Coated and Uncoated Al₂O₃/TiC Sliders in Ultra High Vacuum," *IEEE Transactions on Magnetics*, Vol.32, No.5, Pt.1, September 1996, pp. 3669-3671.
- [39] Chen, C. Y., "Tribochemistry of the Decomposition Mechanisms of Perfluoropolyether Lubricants at the Head-Disk Interface of Hard Disk Drives in UHV," *Ph.D. Thesis 99-003 (Gold Series)*, Computer Mechanics Laboratory, University of California, Berkeley, CA, Fall 1999.
- [40] Wang, R. H., White, R. L., Meeks, S. W., Min, B. G., Kellock, A., Homola, A., Yoon D., "The Interaction of Perfluoro-Polyether Lubricant with Hydrogenated Carbon," *IEEE Transactions on Magnetics*, Vol. 32, No. 5, September 1996, pp. 3777-3779.
- [41] Ruhe, J., Novotny, V., Clarke, T., and Street, G. B., "Ultrathin Perfluoropolyether Films – Influence of Anchoring and Mobility of Polymers on the Tribological Properties," *Journal of Tribology*, Vol. 118, July 1996, pp. 663-668.
- [42] Ma, X., Gui, J., Grannen, K. J., Smoliar, L. A., Marchon, B., Jhon, M. S., and Bauer, C. L., "Spreading of PFPE lubricants on carbon surfaces: effect of hydrogen and nitrogen content," *Tribology Letters*, Vol. 6, 1999, pp. 9-14.
- [43] Pacansky, J., Waltman, R. J., and Pacansky, G., "Electron Beam Induced Degradation of Poly(perfluoropolyethers) and Poly(olefin sulfones)," *Chem. Mater.*, Vol. 5, 1993, pp. 1526-1532.

- [44] Lin, J. L., Bhatia, C. S., Yates, Jr., J. T., "Thermal and Electron-stimulated Chemistry of Fomblin-Zdol Lubricant on a Magnetic Disk," *J. Vac. Sci. Technol. A*, Vol. 13, No. 2, March/April 1995, pp. 163-168.
- [45] Pit, R., Marchon, B., Meeks, S., and Velidandla, V., "Formation of Lubricant "Moguls" at the Head/Disk Interface," *Tribology Letters*, Vol. 10, No. 3, 2001, pp. 133-142.
- [46] Wang, R. H., Meeks, S. W., White, R. L., and Weresin, W. E., "The Effect of Hydrogen in Carbon Overcoats on the Tribology of the Head-disk Interface," *IEEE Transactions on Magnetics*, Vol. 31, No. 6, Pt. 1, November 1995, pp.2919-2921.
- [47] Waltman, R. J., Pocker, D. J., Tyndall, G. W., "Studies on the Interactions Between ZDOL Perfluoropolyether Lubricant and the Carbon Overcoat of Rigid Magnetic Media," *Tribology Letters*, Vol. 4, 1998, pp. 267-275.
- [48] Waltman, R. J., Tyndall, G. W., Pacansky, J., Berry, R. J., "Impact of Polymer Structure and Confinement on the Kinetics of Zdol 4000 Bonding to Amorphous-hydrogenated Carbon," *Tribology Letters*, Vol. 7, 1999, pp. 91-102.
- [49] Waltman, R. J., "Experimental and Theoretical Investigation of the Effect of Lubricant Structure on the Bonding Kinetics of Perfluoroalkylethers on CH_x Amorphous Hydrogenated Carbon," *Chem. Mater.*, Vol. 12, 2000, pp. 2039-2049.
- [50] Waltman, R. J., "Computer-modeling Study of the Interactions of Zdol with Amorphous Carbon Surfaces," *Langmuir*, Vol. 15, 1999, pp. 6470-6483.
- [51] Kasai, P. H. and Spool, A. M., "Z-DOL and Carbon Overcoat: Bonding Mechanism," *IEEE Transactions on Magnetics*, Vol. 37, No. 2, March 2001, pp. 929-933.
- [52] Kasai, P. H., Wass, A., and Yen, B. K., "Carbon Overcoat: Structure and Bonding of Z-DOL," *Journal of Information Storage and Processing Systems*, Vol. 1, No. 3, July 1999, pp. 245-58.
- [53] Lo, R. and Bogy, D. B., "On the Measurements of Nano-hardness and Elastic Modulus of Ultra-thin Overcoats: Effect of W-doping and Annealing on the Properties of DLC," *Technical Report 97-017 (Blue Series)*, Computer Mechanics Laboratory, University of California, Berkeley, CA, September 1997.
- [54] Meeks, S. W., Weresin, W. E., and Rosen, H. J., "Optical Surface Analysis of the Head-Disk-Interface of Thin Film Disks," *Journal of Tribology*, Vol. 117, No. 1, January 1995, pp. 112-118.
- [55] Yun, X. H. and Bogy, D. B., "Tribochemical Study of Hydrogenated and Nitrogenated Overcoats at the Head Disk Interface in Magnetic Disk Drives," *Doctoral Dissertation 96-002 (Gold Series)*, Computer Mechanics Laboratory, University of California, Berkeley, CA, June 1996.
- [56] Wienss, A., Persch-Schuy, G., Hartmann, R., Joeris, P., and Hartmann, U., "Subnanometer scale tribological properties of nitrogen containing carbon coatings used in magnetic storage devices," *J. Vac. Sci. Technol. A*, Vol. 18, No. 4, Jul/Aug 2000, pp. 2023-2026.
- [57] Ma, X., Gui, J., Marchon, B., Jhon, M. S., Bauer, C. L., and Rauch, G. C., "Lubricant Replenishment on Carbon Coated Discs," *IEEE Transactions on Magnetics*, Vol. 35, No. 5, September 1999, pp. 2454-2456.
- [58] Kasai, P. H. and Spool, A. M., "Z-DOL and Carbon Overcoat: Bonding Mechanisms," *IEEE Transactions on Magnetics*, Vol. 37, No. 2, March 2001, pp. 929-933.

- [59] Yanagisawa, M., "Adsorption of Perfluoro-Polyethers on Carbon Surfaces," *Tribology and Mechanics of Magnetic Storage Systems*, Vol. IX, 1994, pp. 25-32.
- [60] Tyndall, G. W., Waltman, R. J., and Pocker, D. J., "Concerning the Interactions between Zdol Perfluoropolyether Lubricant and an Amorphous-Nitrogenated Carbon Surface," *Langmuir*, Vol. 14, 1998, pp. 7527-7536.
- [61] Paserba, K., Shukla, N., Gellman, A. J., Gui, J., and Marchon, B., "Bonding of Ethers and Alcohols to a-CN_x Films," *Langmuir*, Vol. 15, 1999, pp. 1709-1715.
- [62] Cornaglia, L. and Gellman, A., "Fluoroether bonding to carbon overcoats," *Journal of Vacuum Science & Technology A*, Vol. 15, No. 5, September - October 1997, pp. 2755-2765.

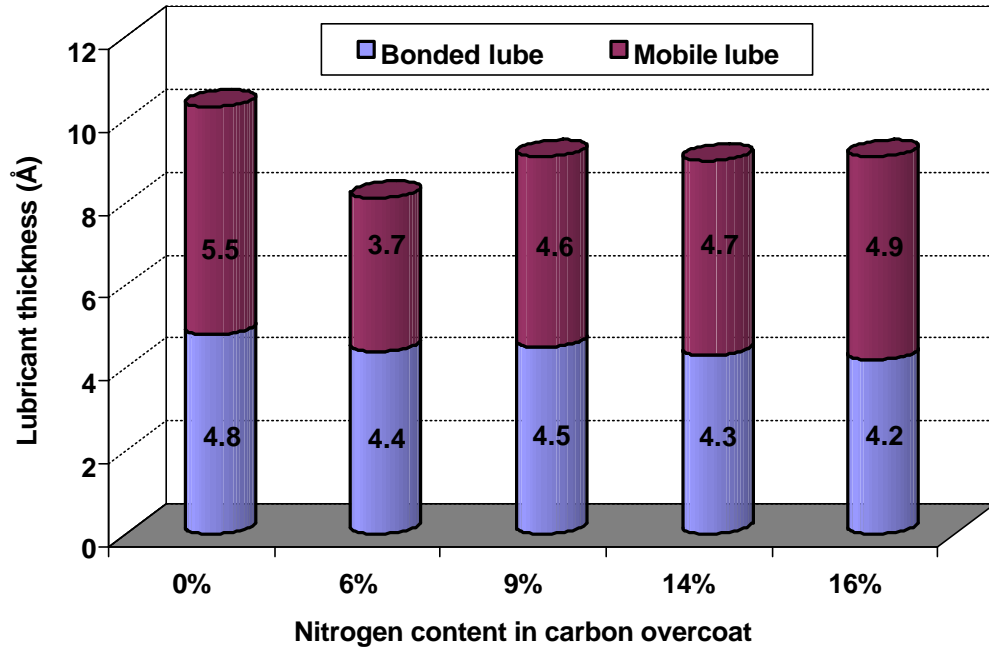


Figure 1. “Bonded” and “mobile” lubricant thicknesses vs. nitrogen content in CN_x overcoat.

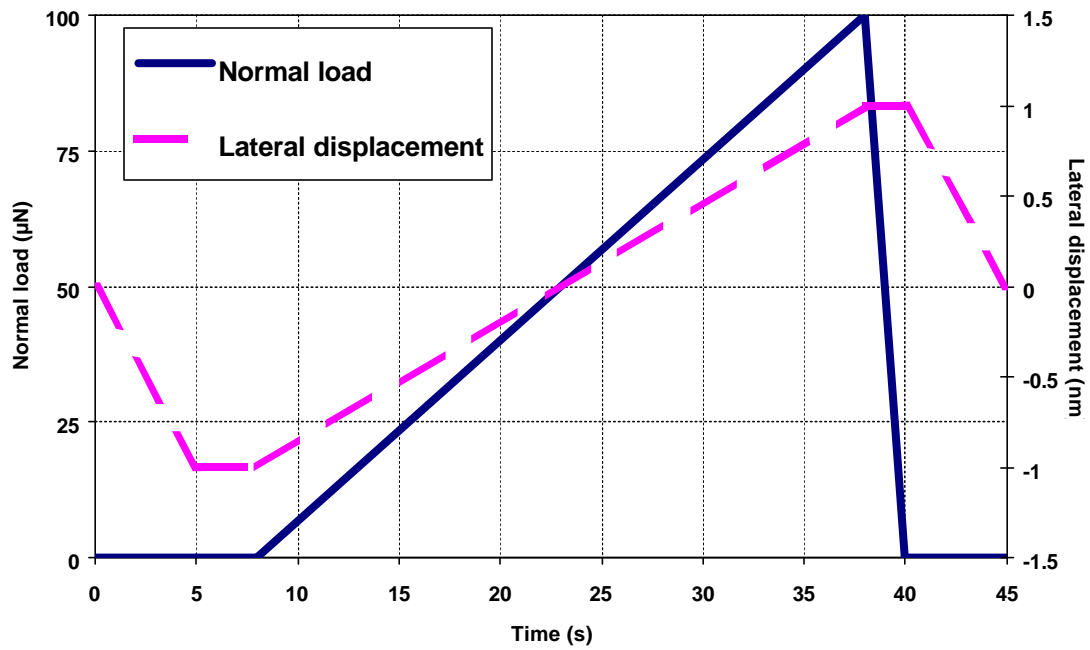


Figure 2. Hysitron nano-scratch test loading and displacement profiles.

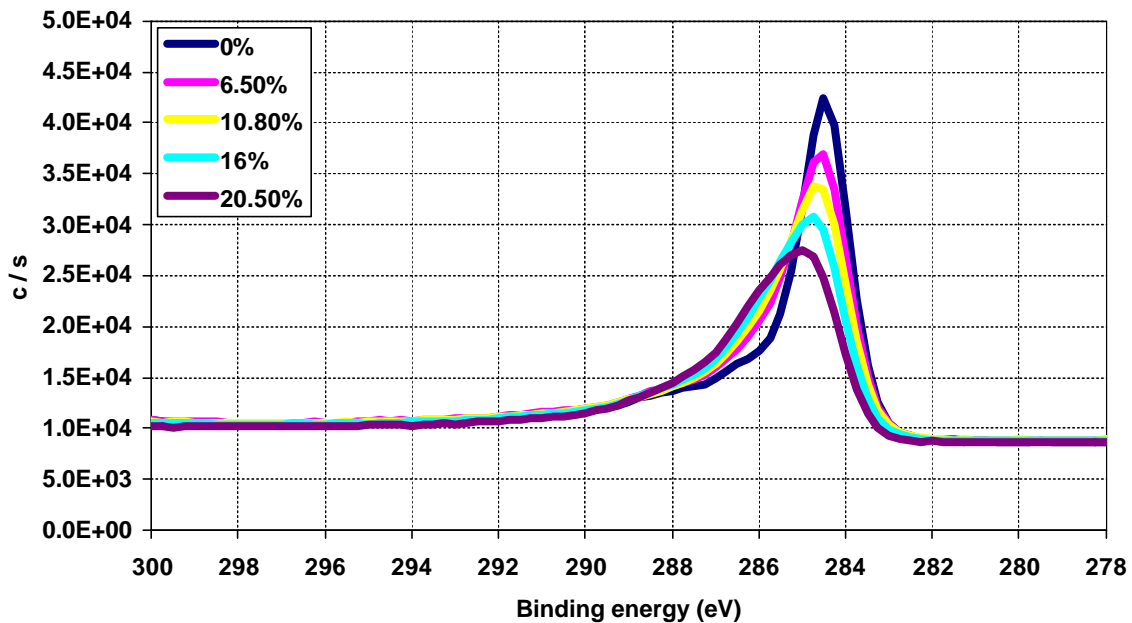


Figure 3. High-resolution C1s spectra of unlubed CN_x overcoat samples.

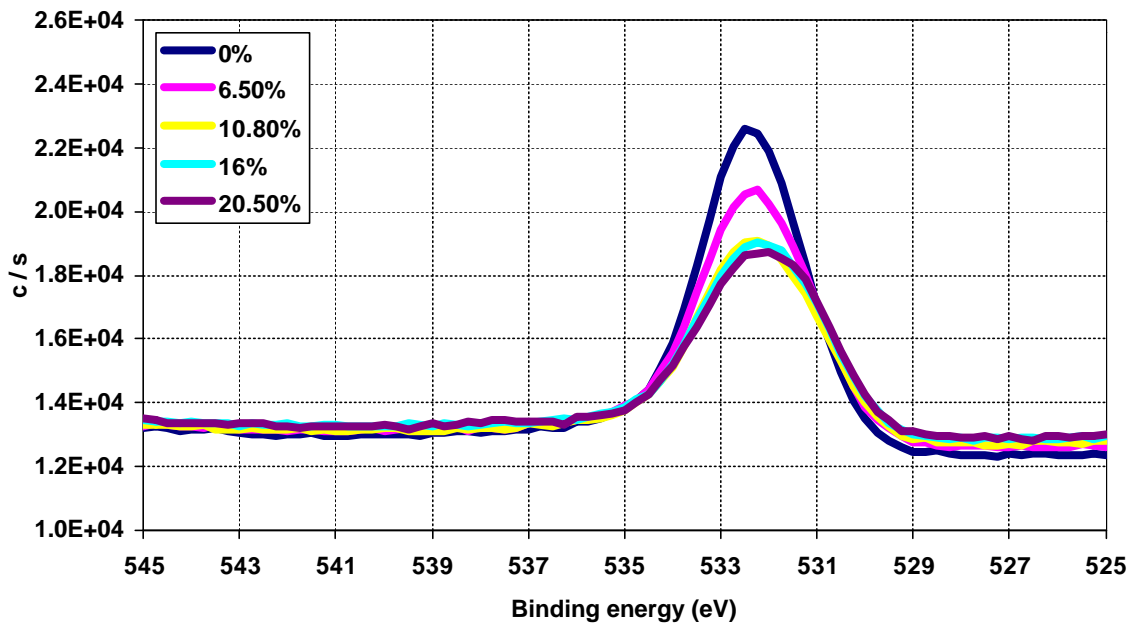


Figure 4. High-resolution O1s spectra of unlubed CN_x overcoat samples.

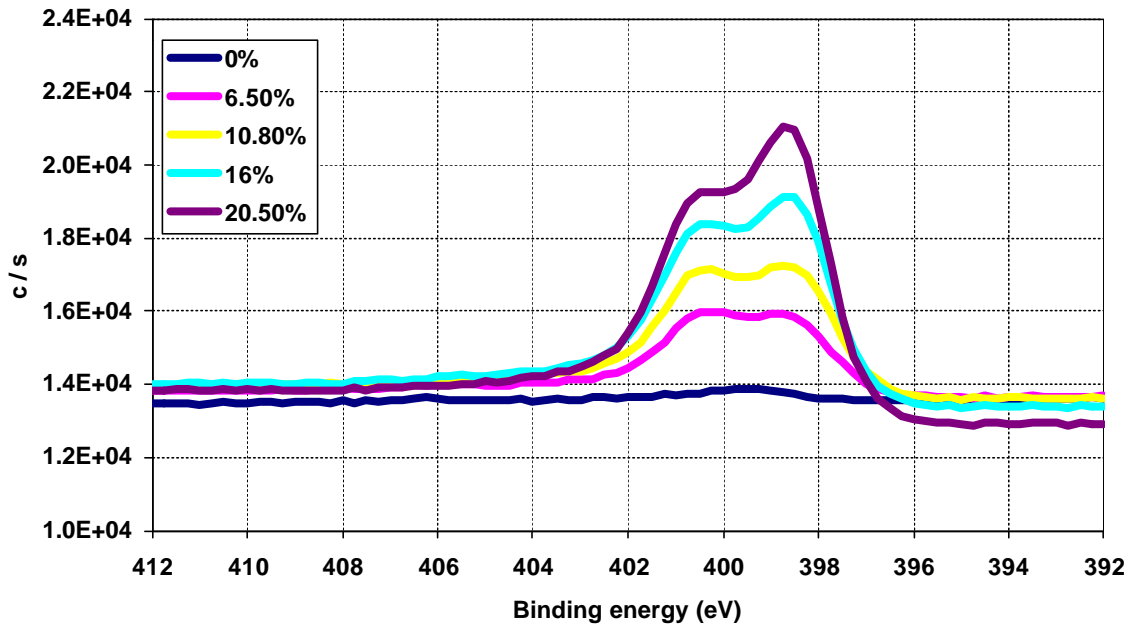


Figure 5. High-resolution N1s spectra of unlubed CN_x overcoat samples.

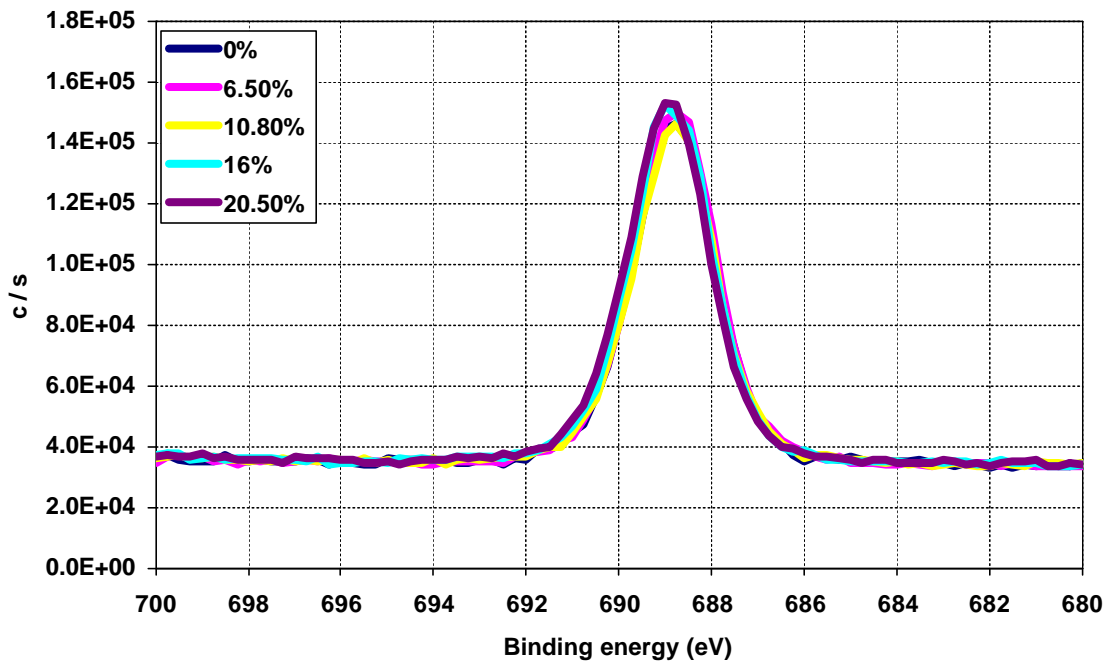


Figure 6. Low-resolution F1s spectra of lubed CN_x overcoat samples.

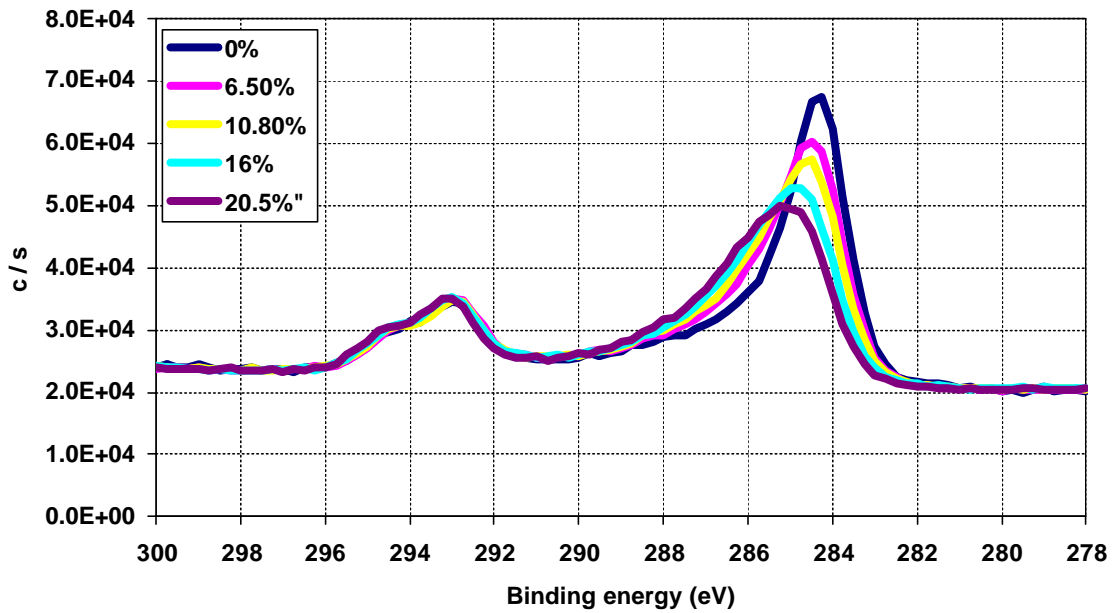


Figure 7. Low-resolution C1s spectra of lubed CN_x overcoat samples.

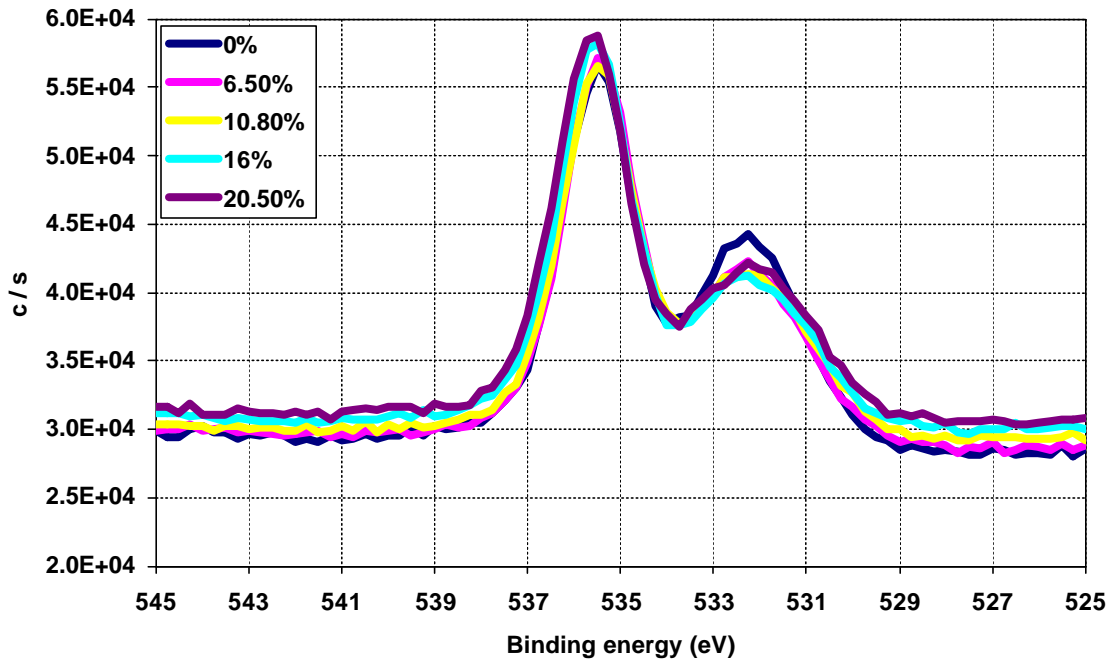


Figure 8. Low-resolution O1s spectra of lubed CN_x overcoat samples.

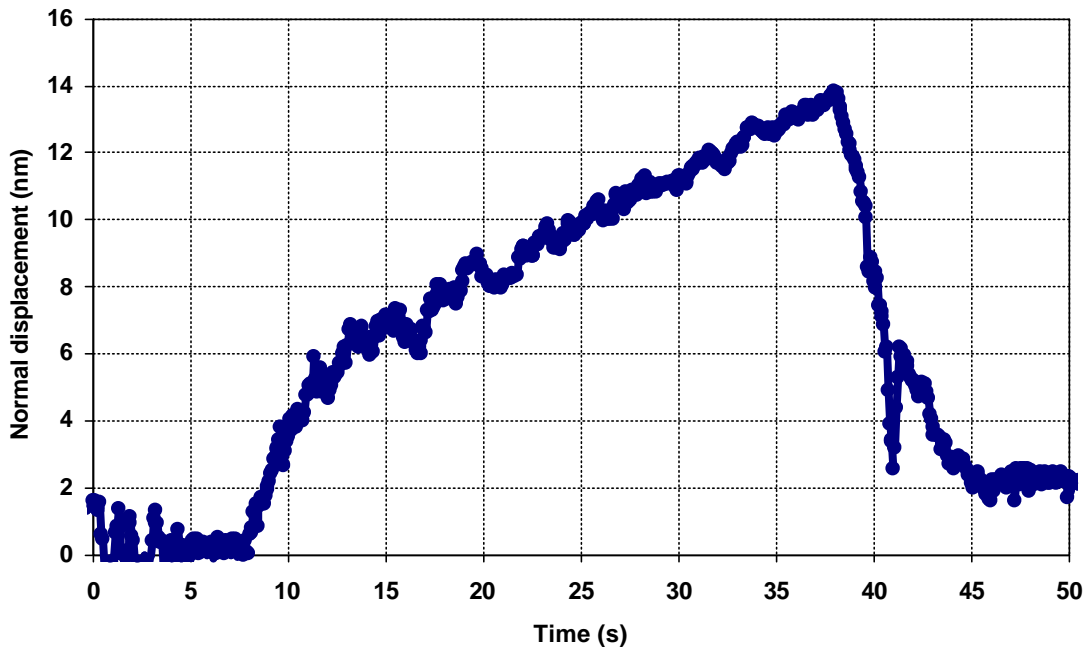


Figure 9. Normal displacement vs. time in Hysitron nano-scratch test of 0% N₂ overcoat sample.

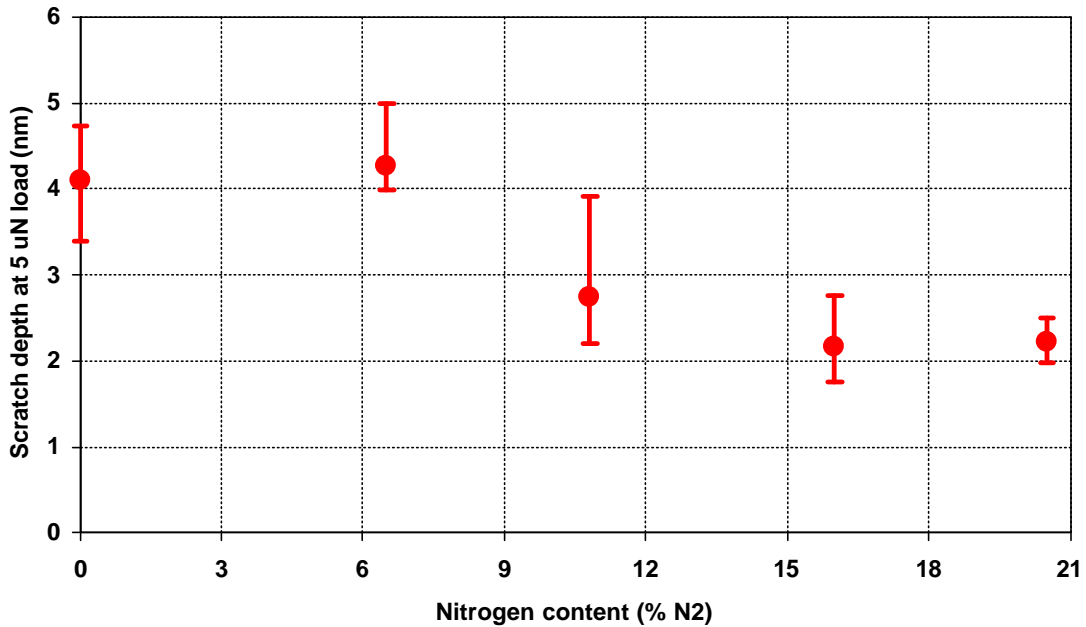


Figure 10. Scratch depth at 5 μ N load vs. nitrogen content in CN_x overcoat in Hysitron nano-scratch tests.

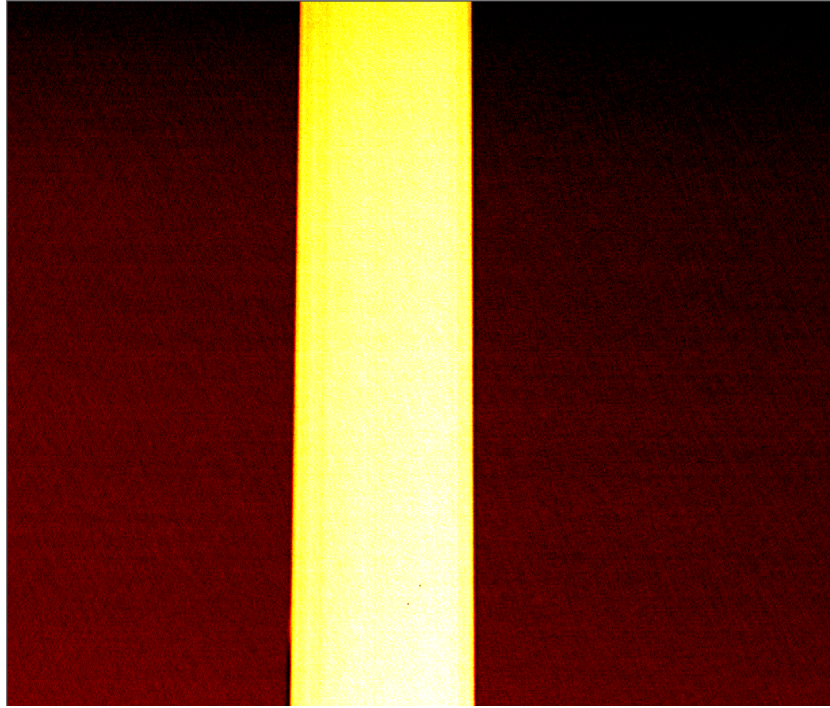


Figure 11. QAbsPhase image of the removed lubricant track from the 18% N₂ disk.

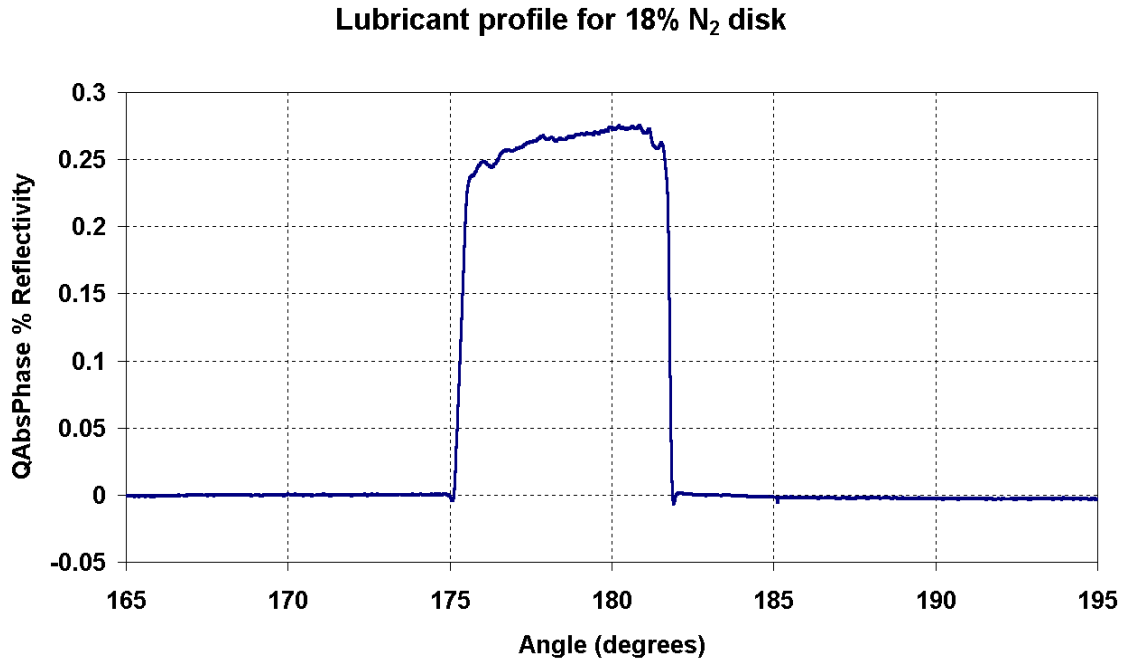


Figure 12. Angular average of QAbsPhase % reflectivity data for the removed lubricant track from the 18% N₂ disk.

18% N₂ disk

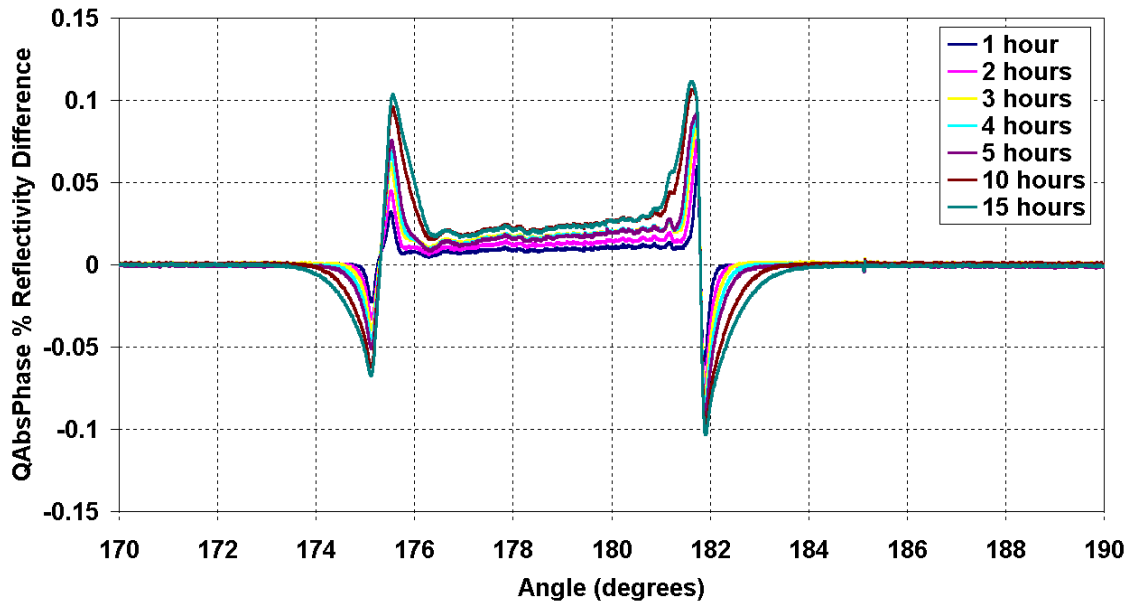


Figure 13. QAbsPhase % reflectivity difference at various time intervals after removal of lubricant from 18% N₂ disk surface. Positive values are associated with re-flow of lubricant, while negative values indicate lubricant removal.

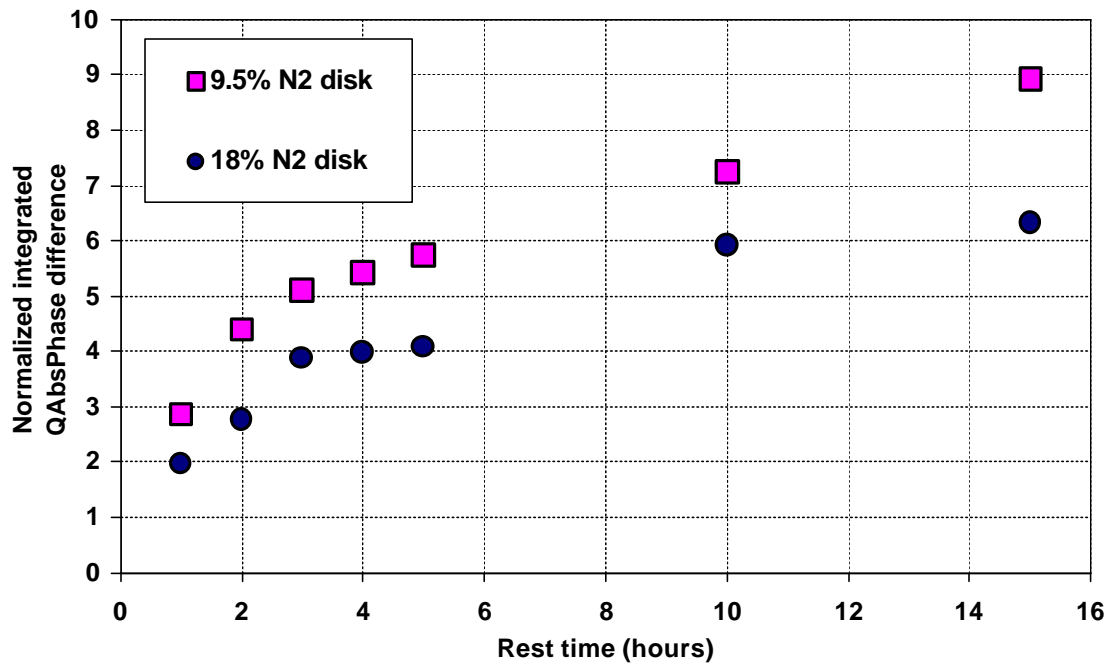


Figure 14. Normalized integrated QAbsPhase difference from test tracks of 9.5 and 18% N₂ disks vs. rest time (hours) after lubricant removal.

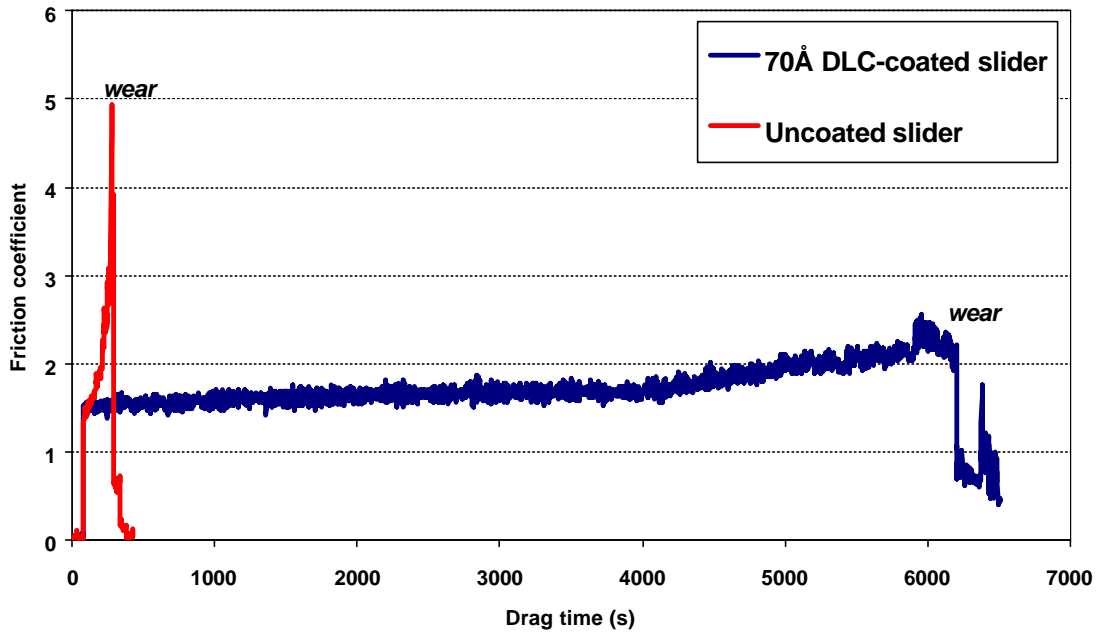


Figure 15. Friction coefficient vs. drag time for 0% N₂ overcoat tested with uncoated and 7 nm DLC-coated sliders.

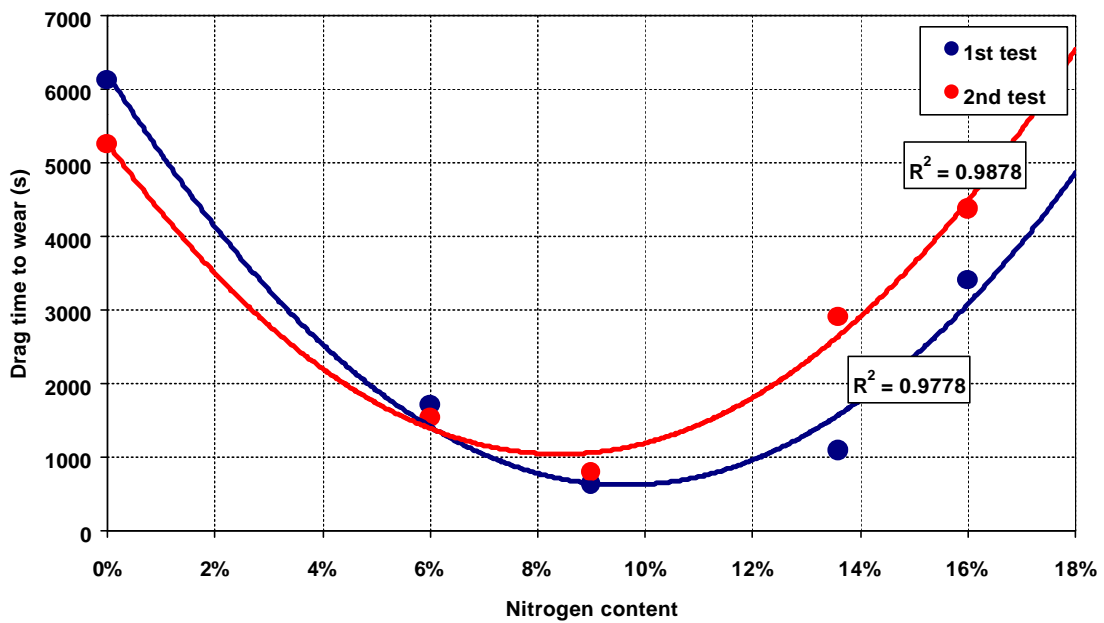


Figure 16. Wear life vs. N₂ content in overcoat for 7 nm DLC-coated slider tests.

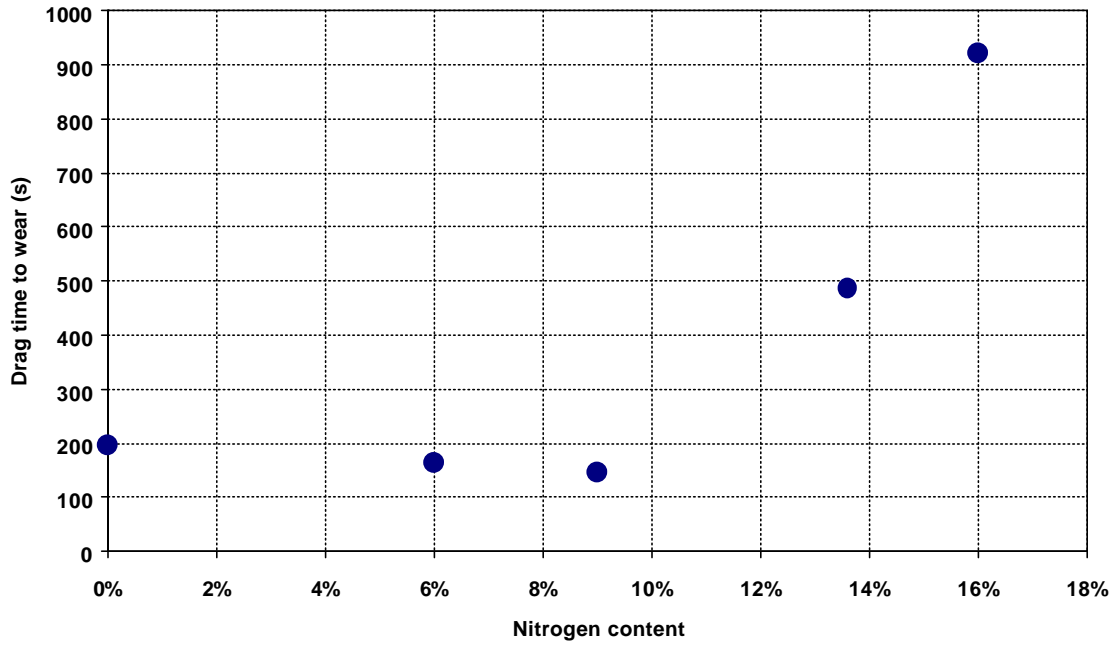


Figure 17. Wear life vs. N_2 content in overcoat for uncoated slider tests.

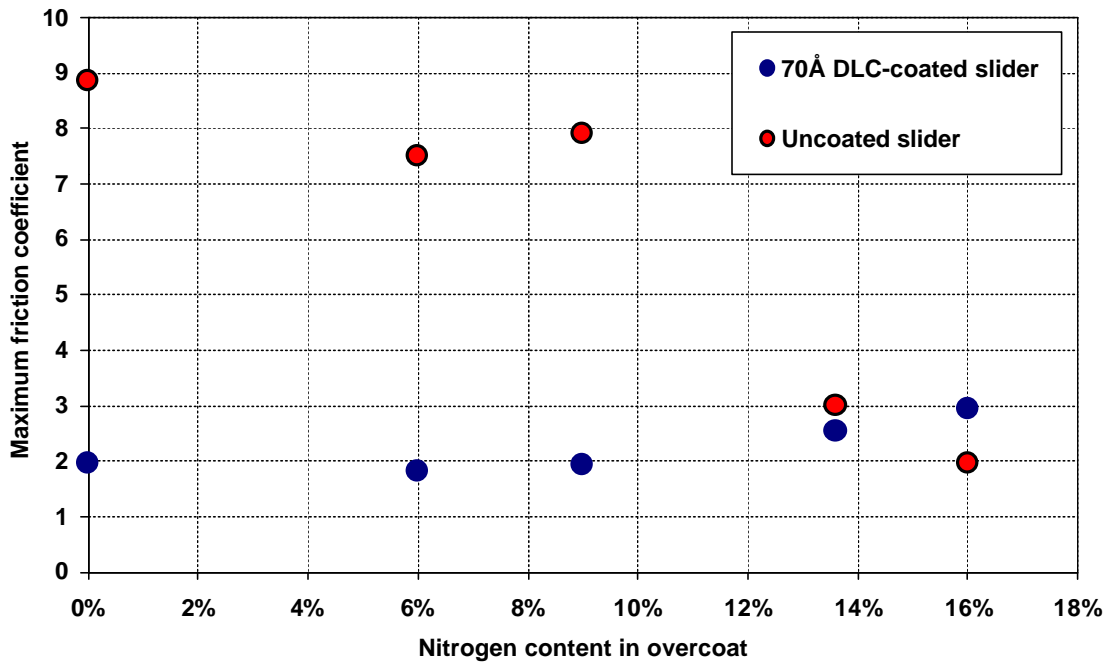


Figure 18. Maximum friction coefficient vs. N_2 content in overcoat for tests with uncoated and 7 nm DLC-coated sliders.

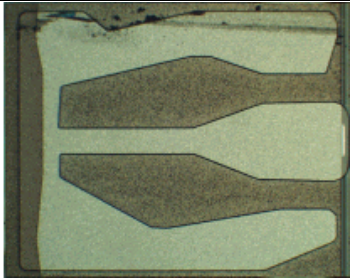
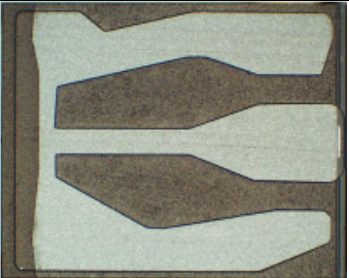
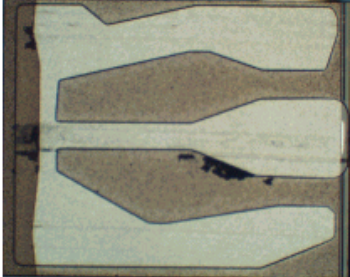
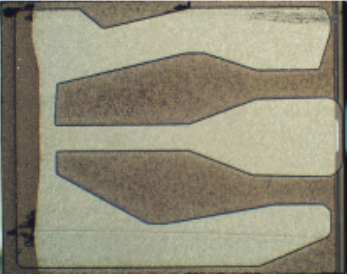
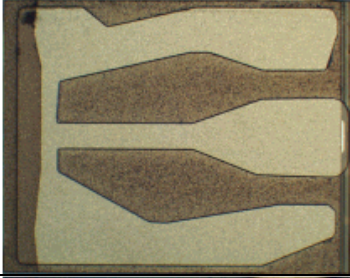
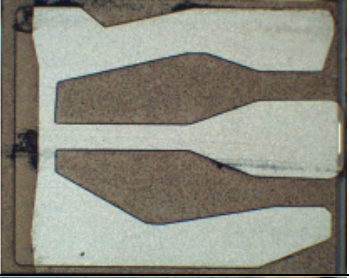
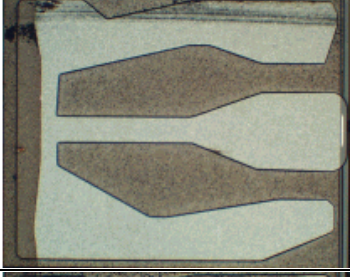
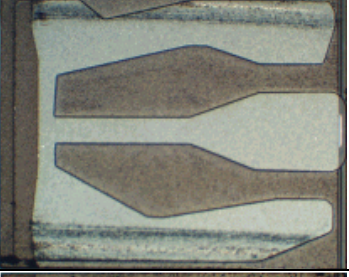
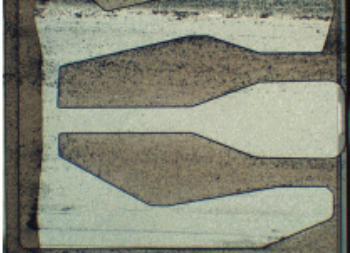
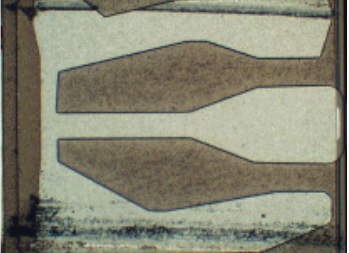
% N ₂ in overcoat	70Å DLC-coated slider	Uncoated slider
0		
6		
9		
13.6		
16		

Figure 19. Microscope pictures of 70Å DLC-coated and uncoated ABS after drag tests.

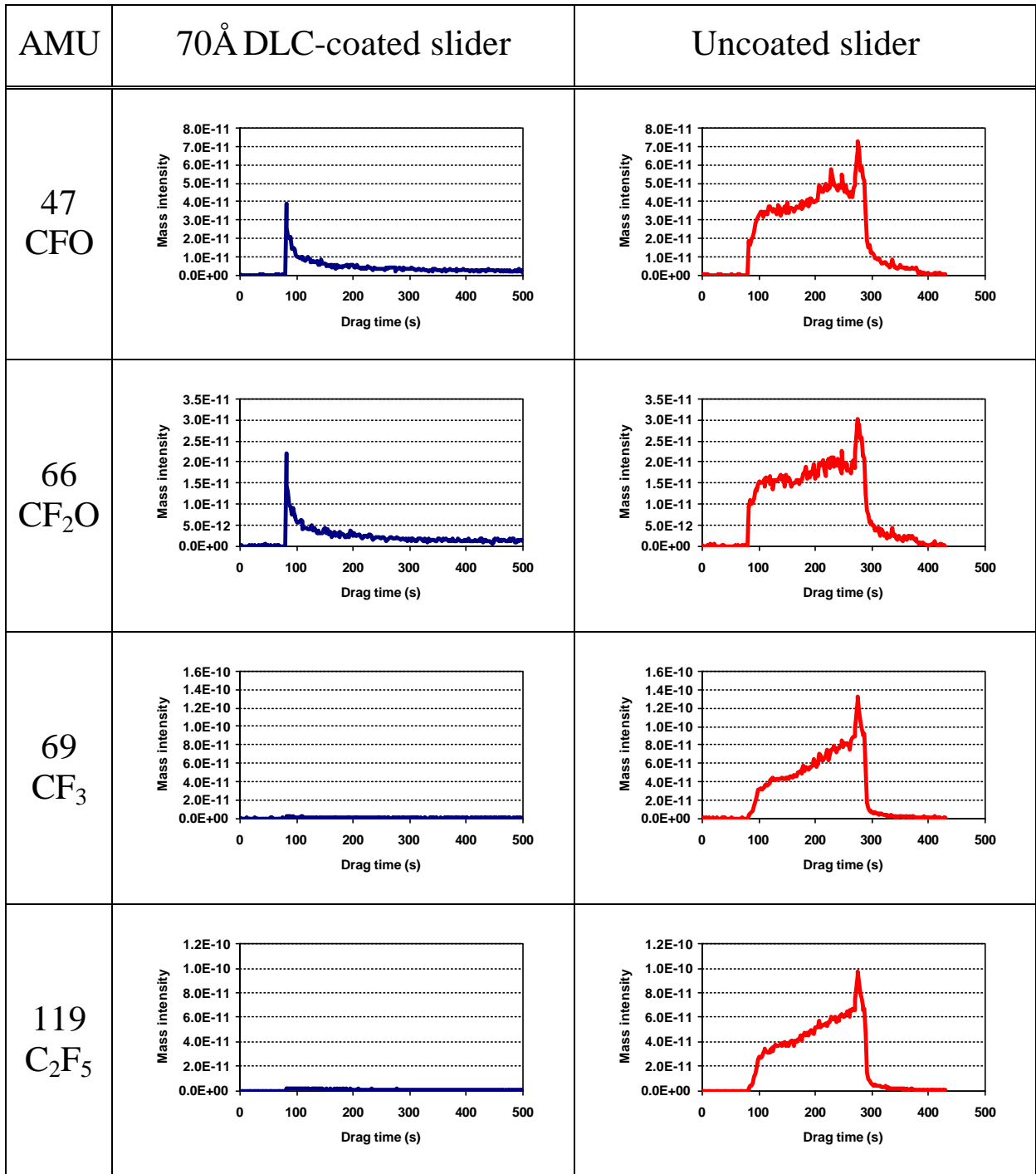


Figure 20. Mass spec data for drag tests with DLC-coated and uncoated sliders on 0% N₂ overcoat disk.

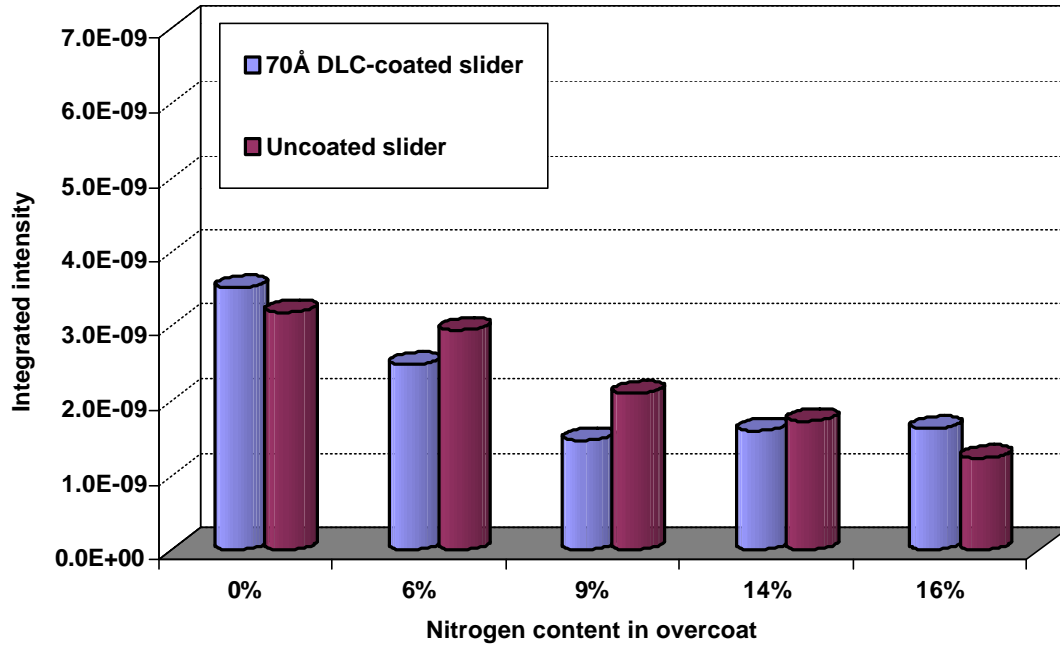


Figure 21. Integrated intensity for CFO (47 a.m.u.) vs. % N₂ in overcoat.

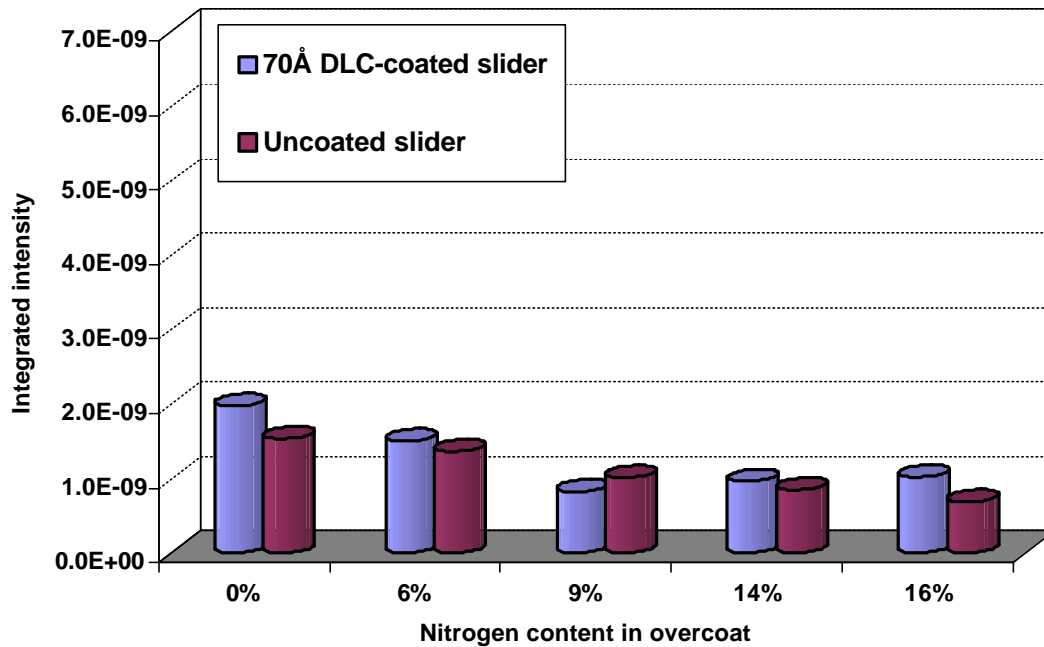


Figure 22. Integrated intensity for CF₂O (66 a.m.u.) vs. % N₂ in overcoat.

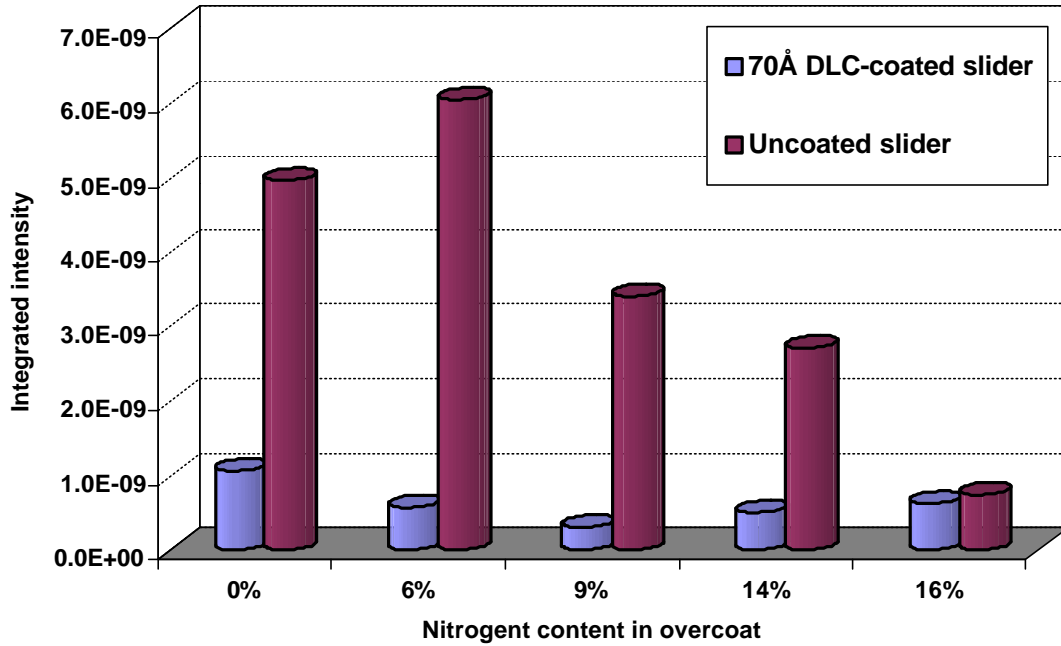


Figure 23. Integrated intensity for CF₃ (69 a.m.u.) vs. % N₂ in overcoat.

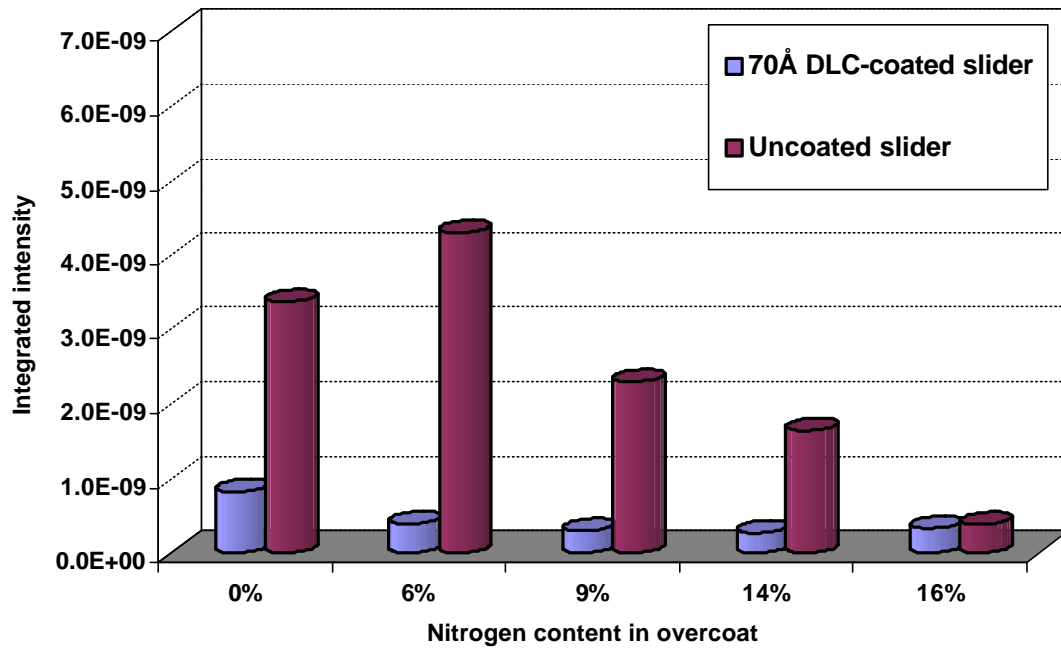


Figure 24. Integrated intensity for C₂F₅ (119 a.m.u.) vs. % N₂ in overcoat.

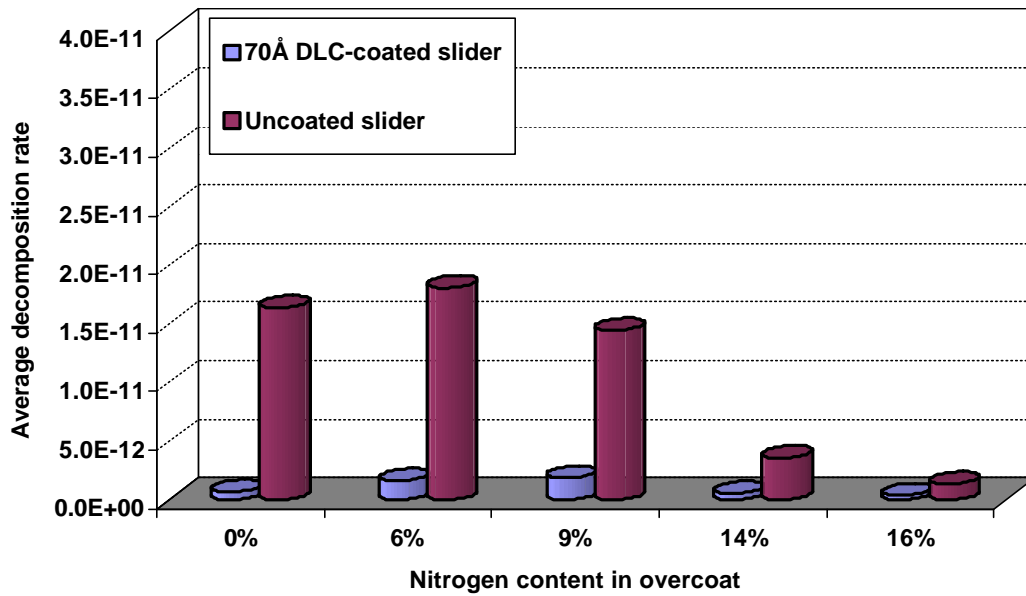


Figure 25. Average decomposition rate for CFO (47 a.m.u.) vs. % N₂ in overcoat.

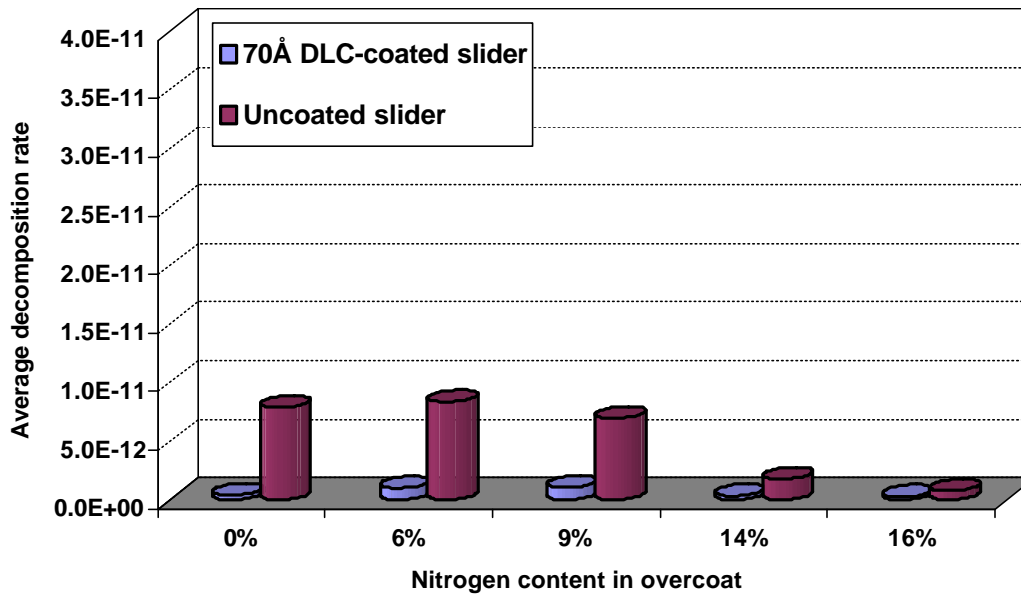


Figure 26. Average decomposition rate for CF₂O (66 a.m.u.) vs. % N₂ in overcoat.

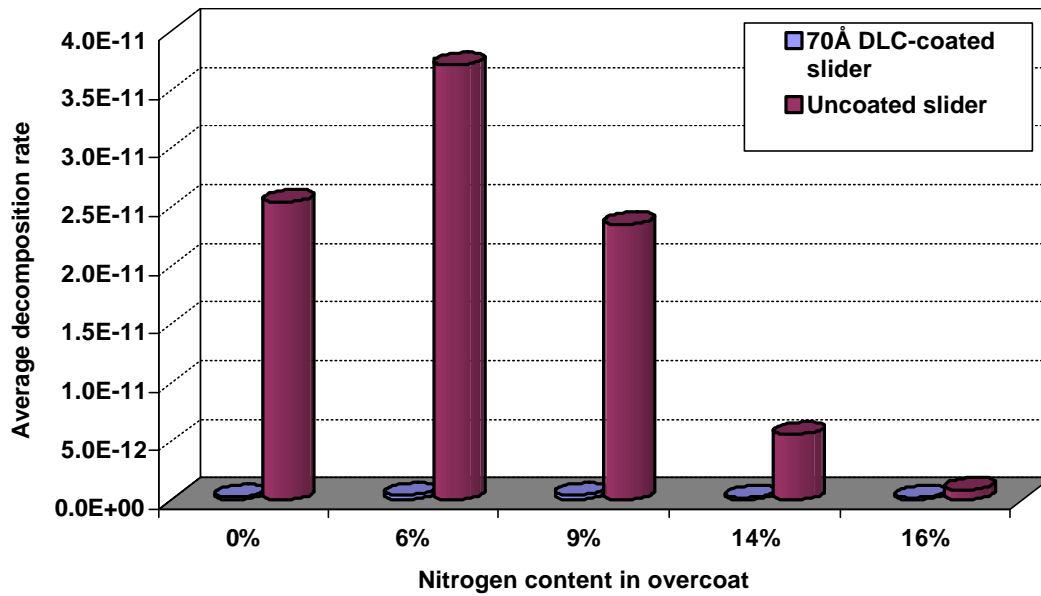


Figure 27. Average decomposition rate for CF_3 (69 a.m.u.) vs. % N_2 in overcoat.

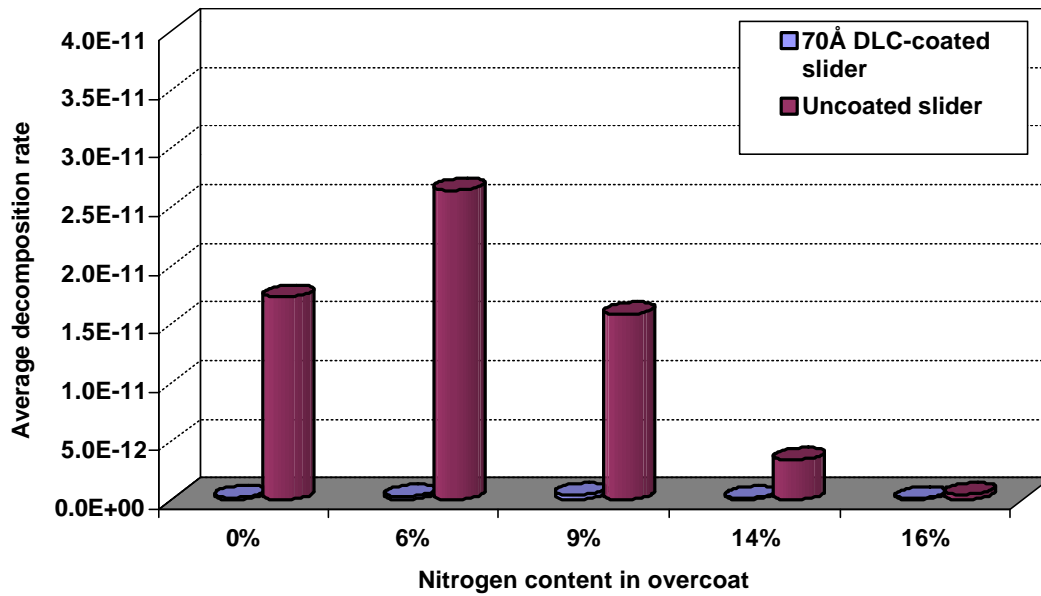


Figure 28. Average decomposition rate for C_2F_5 (119 a.m.u.) vs. % N_2 in overcoat.

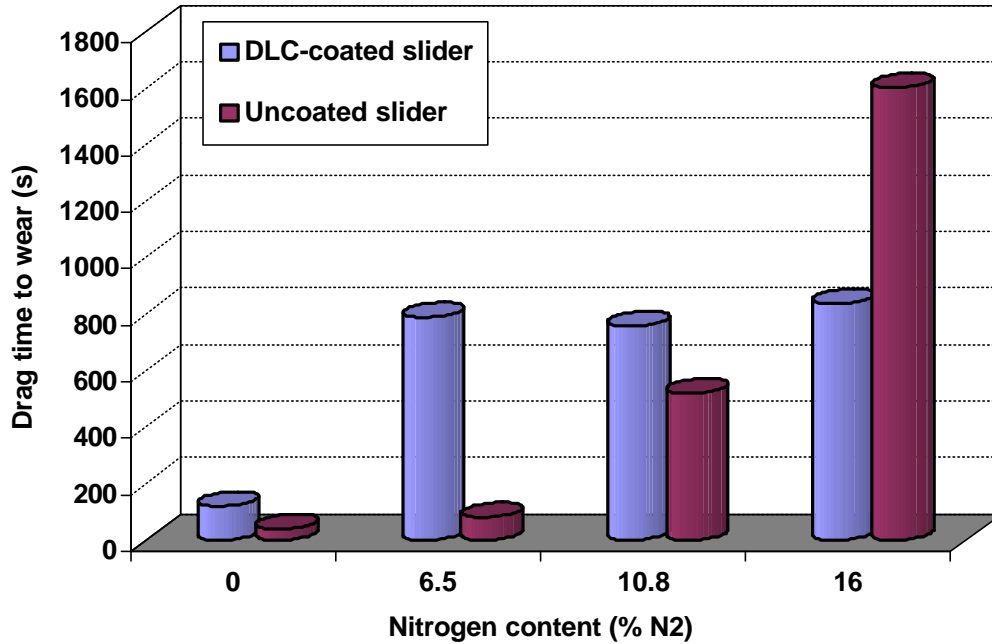


Figure 29. Wear life vs. nitrogen content for unlubricated CN_x disks.

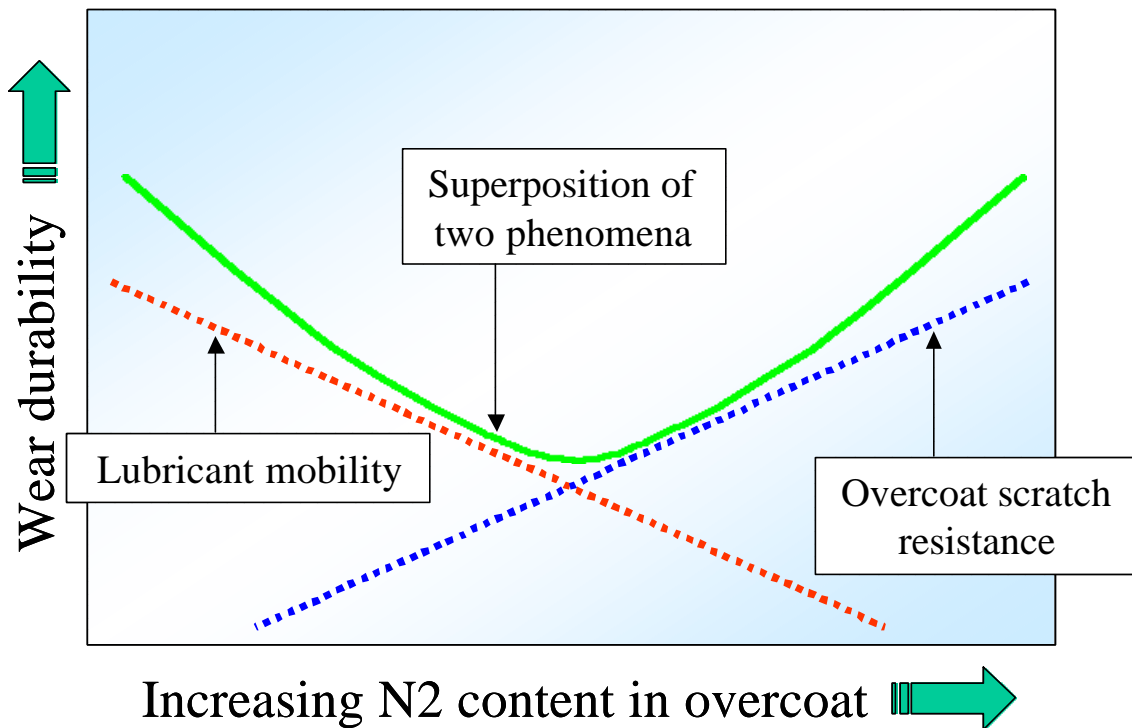


Figure 30. Schematic of material and lubricant properties dependent upon % N₂ in CN_x overcoat.